Supporting Information

Effect of Donor-Acceptor Substituents on the Photophysics of 4-Ethynyl 2,1,3-benzothiadiazole Derivatives

Asit Kumar Pradhan, Manaswini Ray, Parthasarathy Venkatakrishnan* and Ashok Kumar Mishra*

Department of Chemistry, Indian Institute of Technology Madras, Chennai 600036, Tamil Nadu, India

Experimental Details.

Synthetic Specifications. All the reagents were used as received without further purification. Tetrahydrofuran (THF) was dried and distilled over sodium-ketyl radical system. Triethylamine (TEA) and *N,N*-Dimethylformamide (DMF) were distilled using potassium hydroxide and calcium hydride, respectively. For reactions, clean oven-dried glasswares were used. The progress of the reactions was monitored by thin layer chromatography (TLC) using Merck silica-gel (60 F_{254}) precoated plates (0.25 mm) and the compound spots were seen with the naked eye under a UV lamp (365 or 254 nm). The crude product obtained was then purified by column chromatography using silica gel (100-200 mesh). A mixture of hexane and chloroform was used as the eluent. The melting points of the compounds were measured by the open capillary method and the values were corrected. JASCO FT/IR-4100 spectrometer was used for recording infrared spectra. [1]H (400 MHz) and ^{13}C (100/125 MHz) NMR spectra were recorded using a Bruker Avance FT-NMR (400 and 500 MHz) spectrometer using CDCl$_3$ with TMS as the internal reference. The reported ^{1}H and ^{13}C NMR spectra were calibrated with the residual proton solvent peak (CDCl$_3$, δ = 7.26 ppm) and residual carbon solvent peak (CDCl$_3$, δ = 77.16 ppm) respectively. High-resolution Q-TOF mass spectrometer was used to obtain the high-resolution mass spectra.

Photophysical Studies. For this, all the solvents used were of spectroscopic grade. Stock solutions of 10^{-3} M for all compounds were prepared in DCM. Then the experimental samples were prepared by evaporating DCM from the required amount of stock solution by purging nitrogen gas and then adding the desired solvent in it.

Instrumentation. UV-visible absorption spectra were recorded with the help of a Shimadzu UV-2600 spectrophotometer using a quartz cuvette (path length 1 cm). The steady-state fluorescence and anisotropy measurements were done using a Horiba Jobin-Yvon FluoroMax-4 fluorescence spectrophotometer with a 150 W xenon lamp as a light source. To maintain the temperature of the fluorimeter cuvette holder, a CORIO CD-300F refrigerated/heating circulator from Julabo was used. Fluorescence lifetime measurements were carried out using a Horiba Jobin Yvon Fluorocube lifetime instrument with time-correlated single photon counting set up in reverse mode. The instrument response function (IRF) was collected using Ludox AS40 colloidal silica solution. The decays were analyzed using IBH DAS6 software. A fit with

$0.99 \leq \chi^2 \leq 1.30$ was considered as a good fit.[1] For multiexponential lifetime decay, the average fluorescence lifetime (τ_{avg}) was calculated by using the following equation:[2]

$$\tau_{avg} = \frac{\sum_1^n \tau_i^2 \alpha_i}{\sum_1^n \tau_i \alpha_i} \tag{S1}$$

Quantum Yield Measurements. The fluorescence quantum yield (Φ_F or Φ) of all the derivatives was measured using the following relation:

$$\phi_u = \phi_r \frac{F_u A_r \eta_u^2 q_r}{F_r A_u \eta_r^2 q_u} \tag{S2}$$

where, 'F' represents the corrected fluorescence peak area, 'A' the absorbance at the excitation wavelength, 'η' the refractive index of the solvent used, 'q' the excitation light intensity, and the subscripts "r" and "u" refer to reference and unknown, respectively. For calculating ϕ of all the compounds in cyclohexane (CyH) and acetonitrile (ACN), anthracene ($\phi = 0.36$ at 350 nm in cyclohexane) was used as a reference standard. For calculating ϕ of **BTDPhNMe$_2$**, coumarin 30 ($\phi_F = 0.67$ at 380 nm in acetonitrile) was used as a reference standard. The radiative (k_r) and non-radiative (k_{nr}) rate constants were calculated using the formulae:

$$k_r = \frac{\Phi}{\tau} \tag{S3}$$

and

$$k_{nr} = \frac{1}{\tau} - k_r \tag{S4}$$

X-ray Crystal Structure Determination. The crystals of **BTDPhPh** and **BTDPh^{t}But** suitable for single crystal X-ray analysis were obtained by slow evaporation of the saturated DCM solution. The transparent crystals were chosen and mounted along its longest dimension. **BTDPhPh** crystals are blocks in shape whereas **BTDPh^{t}But** are of flake type. The X-ray diffraction data for both **BTDs** (**BTDPhPh** and **BTDPh^{t}But**) were collected on Bruker Axs (Kappa Apex 2) CCD diffractometer equipped with a graphite monochromated Mo Kα ($\lambda = 0.71073$ Å) radiation source at 296 K. The data was integrated using SAINT PLUS and absorption correction was done using multi-scan absorption correction method (SADABS).[3] The structures were solved by direct method (SHELXS-97) and were refined using SHELXL-2018/3 program. All non-hydrogen atoms were refined anisotropically. The direct current (DC) magnetic measurement was performed on vibrating sample magnetometer at variable temperature. The crystallographic table and refinement parameters are provided in Tables S2 and S3 for **BTDPhPh** and **BTDPh^{t}But**, respectively.

Theoretical Calculations. The computational calculations were performed using the Gaussian 16 computational package. Optimization of the ground state of the compounds was carried out using density functional theory (DFT) with B3LYP hybrid functional and 6-311+g(d,p) basis

set without any symmetry constrains. Vibrational analyses were carried out to ascertain the absence of imaginary frequencies. The effect of solvent was included through self-consistent reaction field (SCRF) using a polarizable continuum model (PCM). Excited state geometries were also optimized using the B3LYP/6-311+g(d,p) combination. Potential energy surface (PES) scans were done using a relaxed redundant coordinate scan system using B3LYP/6-311+g(d,p). TD-DFT calculations for both absorption and emission were done using the CAM-B3LYP functional and the same basis set. The electron density difference (EDD) between the excited state and the ground state $[\Delta\rho(r) = \rho^{S_1}(r) - \rho^{S_0}(r)]$ were calculated using Multiwfn software, where ρ^{S_1} and ρ^{S_0} must have the same geometry. $\Delta\rho$ can be divided into positive ($\rho+$) and negative ($\rho-$) parts, which indicate the regions where electron density has increased and decreased, respectively, after excitation. t-index is a measure of CT character in a molecule and is given by:[4]

$$t_{index} = D_{index} - H_{CT} \qquad (S5)$$

where D index (or d_{CT}) is the distance between the two barycenters of $\Delta\rho$ ($\rho+$ and $\rho-$) or the total CT length and H_{CT} is the average degree of spatial extension of $\rho+$ and $\rho-$ in CT direction. If t-index is less than 0, it means that $\rho+$ and $\rho-$ are not considerably separated due to CT. A positive value of t-index implies a significant separation of $\rho+$ and $\rho-$ distributions due to CT and the transition should be identified as a typical CT transition.

Electrochemical Studies. Electrochemical measurements were done at room temperature (25 ± 1 °C) using the electrochemical workstation (CH Instruments 660A) at a scan rate of 0.1 V/s using three electrode system i.e., glassy carbon as working electrode, platinum wire as counter electrode, and Ag/AgCl, KCl (saturated) as reference electrode. All the experiments were done in distilled and nitrogen-purged acetonitrile (ACN) as the solvent using tetra-*n*-butylammonium hexafluorophosphate ([*n*-Bu$_4$N][PF$_6$], 0.1 M) as the non-aqueous supporting electrolyte. All the cyclic voltammograms were calibrated using ferrocene (Fc) as the external standard for each experiment and were corrected. The concentration of the analyte dyes was ca. 1 mM.

Fluorescence Anisotropy Studies. The fluorescence anisotropy value (r) is given by the equation:[5]

$$r = \frac{I_\parallel - I_\perp}{I_\parallel + 2I_\perp} \qquad (S6)$$

Where $I_\parallel$ and $I_\perp$ are intensities of the emitted light parallel and perpendicular to the direction of the polarized excitation light, respectively. Time-resolved fluorescence anisotropy is given by:

$$r(t) = r_\infty + (r_0 - r_\infty)\, exp\left(\frac{-t}{\theta}\right) \qquad (S7)$$

where r_0, r_∞, and θ are the fundamental anisotropy, limiting/residual anisotropy, and rotational correlation time. If the molecule is totally free to rotate, the r_∞ value of zero is obtained. If there is hindered rotation, i.e., the fluorophore is not fully free to rotate, a non-zero limiting anisotropy value is obtained.

General procedure for Sonogashira Coupling: To an oven-dried two-neck round bottomed flask equipped with a reflux condenser and a magnetic stir-bar, 4-bromo-2,1,3-benzothiadiazole (1.0 equivalent) and a solvent mixture of THF and TEA (2:1, v/v) (or DMF and TEA mixture, 2:1, v/v) were added. The resulting solution was degassed with nitrogen gas for 5-7 minutes. Then, the respective alkyne (1.0 equivalent), CuI (5 mol %), and the catalyst Pd(PPh$_3$)$_2$Cl$_2$ (4 mol % relative to the bromo derivative) were added, and the whole solution was again degassed with nitrogen gas for 15 minutes. Later, the temperature was raised to 70 °C, and stirring was continued for about 10-12 hours. The progress of the reaction was monitored using TLC. After the disappearance of the alkyne starting material, the reaction contents were cooled to room temperature, the solvents were evaporated, water was added and the organic contents were extracted with chloroform or ethyl acetate (3 times). The combined organic layer was washed with brine solution to remove the inorganic impurities, then dried over anhydrous sodium sulphate, filtered and the solvent was evaporated. The crude product was purified by silica-gel column chromatography using hexane and chloroform as the eluting solvents.

*4-((4-Nitrophenyl)ethynyl)benzo[c][1,2,5]thiadiazole (**BTDPhNO$_2$**)*
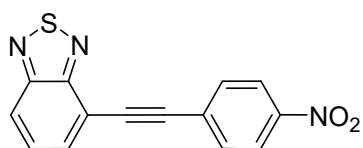
4-Bromobenzothiadiazole (0.35 g, 1.63 mmol) and 1-ethynyl-4-nitrobenzene (0.36 g, 2.45 mmol) were Sonogashira-coupled in presence of Pd(PPh$_3$)$_2$Cl$_2$ (0.057 g, 0.08 mmol) and CuI (0.016 g, 0.08 mmol) in THF (4 mL) and TEA (2 mL) solvent mixture (2:1, v/v) at 70 °C. Time: 12 h.; Yield: 0.252 g, 55%; TLC: R_f = 0.46 (1:1, hexane/chloroform); light yellow solid; MP: 145-147 °C; ^{1}H NMR (400 MHz, CDCl$_3$): δ (ppm) 8.27 (d, J = 8.8 Hz, 2H), 8.08 (d, J = 8.8 Hz, 1H), 7.86 (d, J = 7.2 Hz, 1H), 7.81 (d, J = 8.8 Hz, 2H), 7.64 (dd, J_1 = 8.8 Hz, J_2 = 7.6 Hz, 1H); ^{13}C NMR (100 MHz, CDCl$_3$): δ (ppm) 154.7, 154.5, 147.6, 133.5, 132.8, 129.6, 129.3, 123.8, 123.0, 116.2, 93.5, 90.0; IR (KBr, cm^{-1}): 3080, 2209, 1593, 1517, 1490, 1340, 1311, 1285, 1271, 1173, 1148, 1105, 901, 853, 831, 808, 800, 749, 684, 517; HR ESI-MS: [C$_{14}$H$_7$N$_3$O$_2$S+H]$^+$ = [M+H]$^+$ calculated m/z = 282.0332; found m/z = 282.0333.

*4-(Benzo[c][1,2,5] thiadiazol-4-ylethynyl)benzonitrile (**BTDPhCN**)*
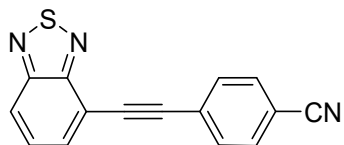
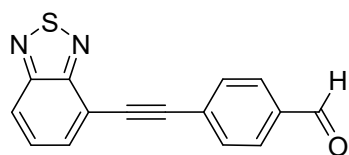4-Bromobenzothiadiazole (0.35 g, 1.63 mmol) and 4-ethynylbenzonitrile (0.31 g, 2.44 mmol) were Sonogashira-coupled in presence of Pd(PPh$_3$)$_2$Cl$_2$ (0.057 g, 0.08 mmol) and CuI (0.016 g, 0.08 mmol) in THF (5 mL) and TEA (2.5 mL) solvent mixture (2:1, v/v) at 70 °C. Time:14 h.; Yield: 0.340 g, 80%; TLC: R$_f$ = 0.34 (1:1, hexane/chloroform); light yellow solid; Mp: 151-153 °C; ^{1}H NMR (400 MHz, CDCl$_3$): δ (ppm) 8.06 (d, J = 8.8 Hz, 1H), 7.84 (d, J = 7.2 Hz, 1H), 7.75 (d, J = 8.0 Hz, 2H), 7.68 (d, J = 8.4 Hz, 2H), 7.63 (dd, J_1 = 6.8 Hz, J_2 = 6.8 Hz, 1H); ^{13}C NMR (100 MHz, CDCl$_3$): δ (ppm) 154.7, 154.5, 133.4, 132.3, 132.2, 129.3, 127.6, 122.9, 118.5, 116.3, 112.3, 93.7, 89.2; IR (KBr, cm^{-1}): 3059, 2224, 1603, 1536, 1499, 1483, 1406, 1351, 1331, 1272, 1178, 1148, 1029, 901, 858, 833, 822, 807, 752, 550, 508, 472. HR ESI-MS: [C$_{15}$H$_7$N$_3$S]$^+$ = [M]$^+$ calculated m/z = 261.0361; found m/z = 261.0385.

*Methyl 4-(benzo[c][1,2,5]thiadiazol-4-ylethynyl)benzoate (**BTDPhCOOMe**)*
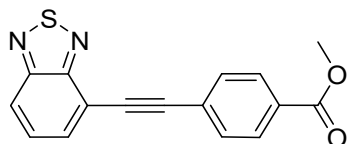
4-Bromobenzothiadiazole (0.35 g, 1.63 mmol) and methyl-4-ethynylbenzoate (0.314 g, 1.96 mmol) were Sonogashira-coupled in presence of Pd(PPh$_3$)$_2$Cl$_2$ (0.057 g, 0.08 mmol) and CuI (0.016 g, 0.08 mmol) in THF (5 mL) and TEA (2.5 mL) solvent mixture (2:1, v/v) at 70 °C. Time: 11 h.; Yield: 0.431 g, 90%; TLC: R$_f$ = 0.34 (1:1, hexane/chloroform); Off-white solid; Mp: 179-181 °C; ^{1}H NMR (400 MHz, CDCl$_3$): δ (ppm) 8.06 (d, J = 8.4 Hz, 2H), 8.03 (d, J = 8.4 Hz, 1H), 7.83 (d, J = 7.2 Hz, 1H), 7.72 (d, J = 8.4 Hz, 2H), 7.608 (dd, J_1 = 7.2 Hz, J_2 = 7.2 Hz, 1H), 3.94 (s, 3H); ^{13}C NMR (100 MHz, CDCl$_3$): δ (ppm) 166.6, 154.7, 154.6, 133.2, 133.1, 132.0, 130.2, 129.7, 129.66, 129.32, 127.4, 122.5, 116.8, 94.8, 87.9, 52.4; IR (KBr, cm^{-1}): 3076, 3062, 3012, 2957, 2212, 1716, 1605, 1537, 1489, 1428, 1403, 1325, 1305, 1272, 1243, 1190, 1174, 1105, 1028, 1015, 959, 901, 854, 830, 805,767, 748, 693. HR ESI-MS: [C$_{16}$H$_{10}$N$_2$O$_2$S+H]$^+$ = [M+H]$^+$ calculated m/z = 295.0536; found m/z = 295.05541.

*4-((6,7-Dihydrobenzo[c][1,2,5] thiadiazol-4-yl)ethynyl)benzaldehyde (**BTDPhCHO**)*

4-Bromobenzothiadiazole (0.35 g, 1.63 mmol) and 4-ethynylbenzaldehyde (0.319 g, 2.45 mmol) were Sonogashira-coupled in presence of Pd(PPh$_3$)$_2$Cl$_2$ (0.057 g, 0.08 mmol) and CuI (0.016 g, 0.08 mmol) in THF (5 mL) and TEA (2.5 mL) solvent mixture (2:1, v/v) at 70 °C. Time: 12 h.; Yield: 0.322 g, 75%; TLC: R$_f$ = 0.31 (1:1, hexane/chloroform); Greenish-yellow solid; Mp: 140-142 °C; ^{1}H NMR (400 MHz, CDCl$_3$): δ (ppm) 10.10 (s, 1H), 8.05 (d, J = 8.8 Hz, 1H), 7.91 (d, J = 8.0 Hz, 2H), 7.85 (d, J = 8.0 Hz, 1H), 7.81 (d, J = 8.8 Hz, 2H), 7.62 (dd, J_1 = 7.2 Hz and J_2 = 7.2 Hz, 1H); ^{13}C NMR (100 MHz, CDCl$_3$): δ (ppm) 191.5, 154.7, 154.5, 136.0, 133.3, 132.6, 129.7, 129.3, 129.0, 122.7, 116.5, 94.6, 88.9; IR (KBr, cm^{-1}): 3062, 2847, 2743, 2207, 1698, 1598, 1560, 1410, 1386, 1354, 1327, 1300, 1287, 1274, 1206, 1162, 1101, 899, 854, 827, 808, 788, 753, 708, 529, 470; HR ESI-MS: [C$_{15}$H$_8$N$_2$OS+H]$^+$ = [M+H]$^+$ calculated m/z = 265.043; found m/z = 265.043.

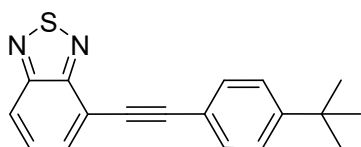*7-(Phenylethynyl)-4,5-dihydrobenzo[c][1,2,5]thiadiazole (**BTDPh**)*
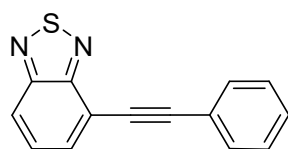
4-Bromobenzothiadiazole (0.35 g, 1.62 mmol) and ethynylbenzene (0.21 mL, 1.96 mmol) were Sonogashira-coupled in presence of Pd(PPh$_3$)$_2$Cl$_2$ (0.057 g, 0.08 mmol) and CuI (0.016 g, 0.08 mmol) in THF (4 mL) and TEA (2 mL) solvent mixture (2:1, v/v) at 70 °C. Time: 12 h.; Yield: 0.312 g, 81%; TLC: R$_f$ = 0.78 (1:1, hexane/chloroform); Yellowish-white solid; Mp: 82-84 °C; ^{1}H NMR (400 MHz, CDCl$_3$): δ (ppm) 8.00 (d, J = 8.8 Hz, 1H), 7.80 (d, J = 7.2 Hz, 1H), 7.68-7.66 (m, 2H), 7.60 (dd, J_1 = 8.8 Hz, J_2 = 7.2 Hz, 1H), 7.40-7.38 (m, 3H); ^{13}C NMR (100 MHz, CDCl$_3$): δ (ppm) 154.7, 154.6, 132.7, 132.1, 129.3, 129.0, 128.5, 122.7, 121.9, 117.3, 95.9, 85.2; IR (KBr, cm^{-1}): 3076, 3060, 3030, 3017, 2217, 1655, 1597, 1536, 1489, 1439, 1327, 1275, 1069, 1031, 970, 921, 901, 853, 831, 803, 759, 750, 693, 587, 533, 513, 490, 408; HR ESI-MS: [C$_{14}$H$_8$N$_2$S+H]$^+$ = [M+H]$^+$ calculated m/z =237.0481; found m/z = 237.0477.

*4-([1,1'-Biphenyl]-4-ylethynyl)benzo[c][1,2,5]thiadiazole (**BTDPhPh**)*
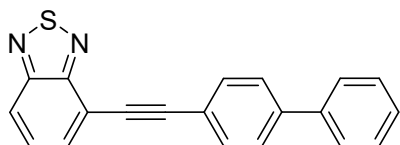
4-Bromobenzothiadiazole (0.35 g, 1.63 mmol) and 4-ethynyl-1,1'-biphenyl (0.349 g, 1.96 mmol) were Sonogashira-coupled in presence of Pd(PPh$_3$)$_2$Cl$_2$ (0.057 g, 0.08 mmol) and CuI (0.016 g, 0.08 mmol) in THF (5 mL) and TEA (2.5 mL) solvent mixture (2:1, v/v) at 70 °C. Time: 13 h.; Yield: 0.381 g, 75%; TLC: R$_f$ = 0.81 (1:1, hexane/chloroform); yellow solid; Mp: 156-158 °C; ^{1}H NMR (400 MHz, CDCl$_3$): δ (ppm) 8.01 (d, J = 8.8 Hz, 1H), 7.82 (d, J = 6.8 Hz, 1H), 7.74 (d, J = 8.0 Hz, 2H), 7.65-7.59 (m, 5H), 7.47 (t, J = 7.2 Hz, 2H), 7.38 (t, J = 7.2 Hz, 1H); ^{13}C NMR (100 MHz, CDCl$_3$): δ (ppm) 154.7, 154.8, 141.7, 140.3, 132.7, 132.5, 129.3, 129.0, 127.9, 127.2, 121.9, 121.6, 117.3, 95.9, 85.9; IR (KBr, cm^{-1}): 3051, 3030, 2205, 1578, 1538, 1519, 1486, 1446, 1402, 1355, 1327, 1140, 1111, 1028, 1004, 901, 858, 838, 815, 804, 766, 745, 717, 692, 681, 510; HR ESI-MS: [C$_{20}$H$_{12}$N$_2$S+H]$^+$ = [M + H]$^+$ calculated m/z =313.0794; found m/z = 313.0803.

*4-((4-(Tert-butyl)phenyl)ethynyl)benzo[c][1,2,5]thiadiazole* (**BTDPh'But**)

4-Bromobenzothiadiazole (0.35 g, 1.63 mmol) and 1-(*tert*-butyl)-4-ethynylbenzene (0.310 g, 1.96 mmol) were Sonogashira-coupled in presence of Pd(PPh$_3$)$_2$Cl$_2$ (0.057 g, 0.08 mmol) and CuI (0.016 g, 0.08 mmol) in THF (5 mL) and TEA (2.5 mL) solvent mixture (2:1, v/v) at 70 °C. Time: 15 h.; Yield: 0.442 g, 93%; TLC: R$_f$ = 0.78 (1:1, hexane/chloroform); bright yellow solid; Mp: 105-107 °C; ^{1}H NMR (400 MHz, CDCl$_3$): δ (ppm) 7.98 (d, J = 8.8 Hz, 1H), 7.79 (d, J = 7.2 Hz, 1H), 7.61-7.56 (m, 3H), 7.41 (d, J = 8.4 Hz, 2H), 1.34 (s, 9H); ^{13}C NMR (100 MHz, CDCl$_3$): δ (ppm) 154.8, 154.7, 152.4, 132.6, 131.8, 129.4, 125.5, 121.6, 119.7, 117.6, 96.2, 84.6, 35.0, 31.3; IR (KBr, cm^{-1}): 2947, 2901, 2862, 2209, 1655, 1584, 1539, 1502, 1483, 1463, 1406, 1389, 1362, 1327, 1265, 1105, 1027, 904, 852, 836, 809, 755, 560, 505. HR ESI-MS: [C$_{18}$H$_{16}$N$_2$S+H]$^+$ = [M+H]$^+$ calculated m/z = 293.1107; found m/z = 293.1118.

4-((4-Methoxyphenyl)ethynyl)benzo[c][1,2,5]thiadiazole (**BTDPhOMe**)
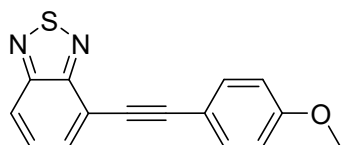
4-Bromobenzothiadiazole (0.35 g, 1.63 mmol) and 1-ethynyl-4-methoxybenzene (0.280 g, 2.12 mmol) were Sonogashira-coupled in presence of Pd(PPh$_3$)$_2$Cl$_2$ (0.057 g, 0.08 mmol) and CuI (0.016 g, 0.08 mmol) in THF (5 mL) and TEA (2.5 mL) solvent mixture (2:1, v/v) at 70 °C. Time: 15 h.; Yield: 0.347 g, 80%; TLC: R$_f$ = 0.59 (1:1, hexane/chloroform); greenish yellow solid; Mp: 127-129 °C; ^{1}H NMR (400 MHz, CDCl$_3$): δ 7.97 (d, J = 8.80 Hz, 1H), 7.77 (d, J = 6.8 Hz, 1H), 7.63-7.56 (m, 3H), 6.92 (d, J = 8.7 Hz, 2H), 3.85 (s, 3H); ^{13}C NMR (100 MHz, CDCl$_3$): δ (ppm) 160.3, 154,8, 154.7, 133.7, 132.4, 129.4, 121.5, 117.7, 114.8, 114.2, 96.2, 84.1, 55.5; IR (KBr, cm^{-1}): 2962, 2915, 2838, 2211, 1604, 1582, 1567, 1536, 1507, 1466, 1456, 1438, 1321, 1290, 1249, 1183, 1170, 1147, 1105, 1051, 1030, 1023, 903, 852, 836, 807, 756, 533, 515, 501, 448; HR ESI-MS: [C$_{15}$H$_{10}$N$_2$OS+H]$^+$ = [M+H]$^+$ calculated m/z = 267.0587; found m/z = 267.0596.

*4-(Benzo[c][1,2,5]thiadiazol-4-ylethynyl)-N,N-dimethylaniline (**BTDPhNMe$_2$**)*
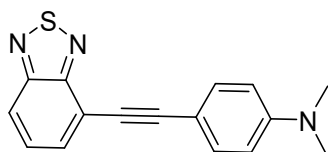
4-Bromobenzothiadiazole (0.35 g, 1.63 mmol) and 4-ethynyl-*N,N*-dimethylaniline (0.284 g, 1.96 mmol) were Sonogashira-coupled in presence of Pd(PPh$_3$)$_2$Cl$_2$ (0.057 g, 0.08 mmol) and CuI (0.016 g, 0.08 mmol) in THF (5 mL) and TEA (2.5 mL) solvent mixture (2:1, v/v) at 70 °C. Time: 14 h.; Yield: 386 g, 85%; TLC: R$_f$ = 0.46 (1:1, hexane/chloroform); brown-yellow solid; Mp: 127-129°C; ^{1}H NMR (400 MHz, CDCl$_3$): δ 7.93 (d, J = 8.8 Hz, 1H), 7.73 (d, J = 6.8 Hz, 1H), 7.58-7.53 (m, 3H), 6.68 (d, J = 7.6 Hz, 2H), 3.01 (s, 6H); ^{13}C NMR (100 MHz, CDCl$_3$): δ (ppm) 154.8.3, 154,7, 150.6, 133.4, 131.8, 129.5, 120.8, 118.3, 111.8, 109.3, 97.9, 83.7, 40.3; IR (KBr, cm^{-1}): 3039, 2997, 2909, 2858, 2807, 2209, 1584, 1536, 1518, 1481, 1442, 1359, 1300, 1228, 1209, 1182, 1169, 1123, 1066, 1035, 1026, 943, 901, 820, 808, 752, 535, 498; HR ESI-MS: [C$_{16}$H$_{13}$N$_3$S+H]$^+$ = [M+H]$^+$ calculated m/z = 280.0903; found m/z = 280.0912.
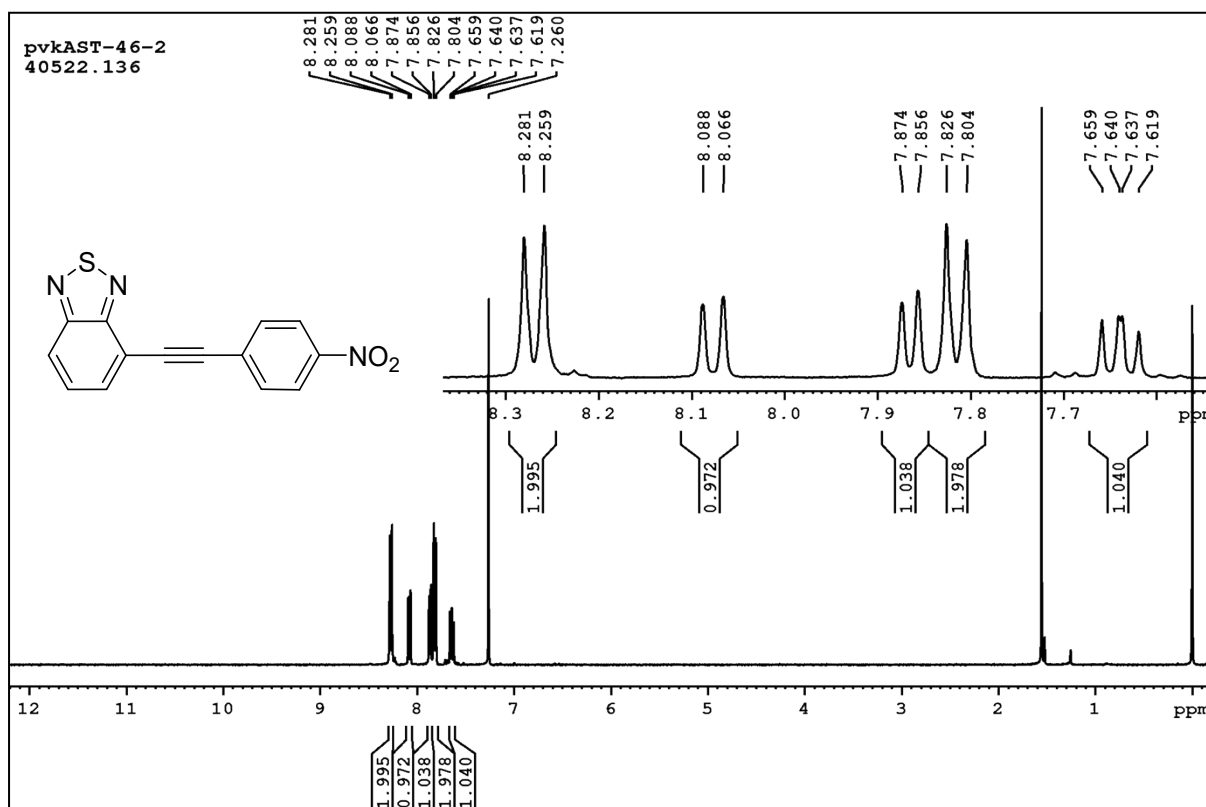
Fig. S1. ^{1}H NMR spectrum of **BTDPhNO$_2$** in CDCl$_3$.
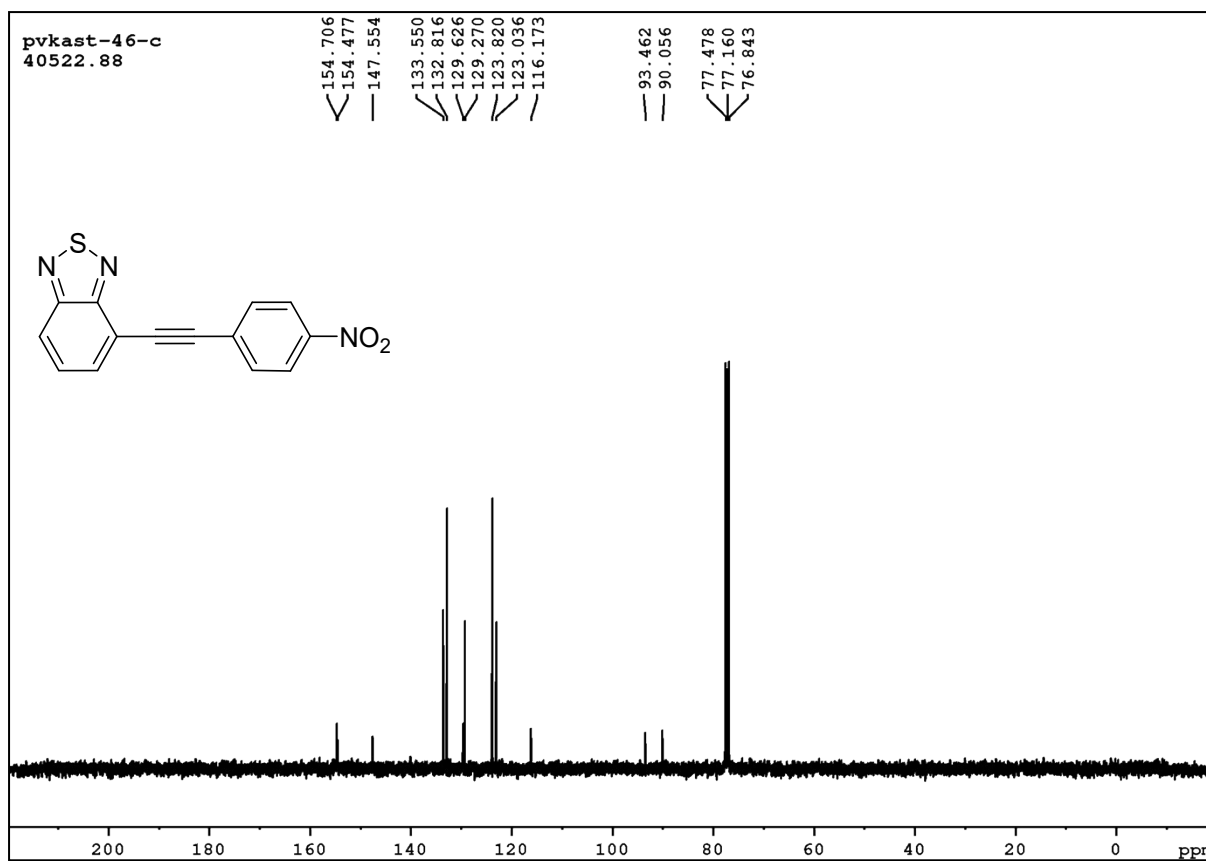
Fig. S2. ^{13}C NMR spectrum of **BTDPhNO$_2$** in CDCl$_3$.
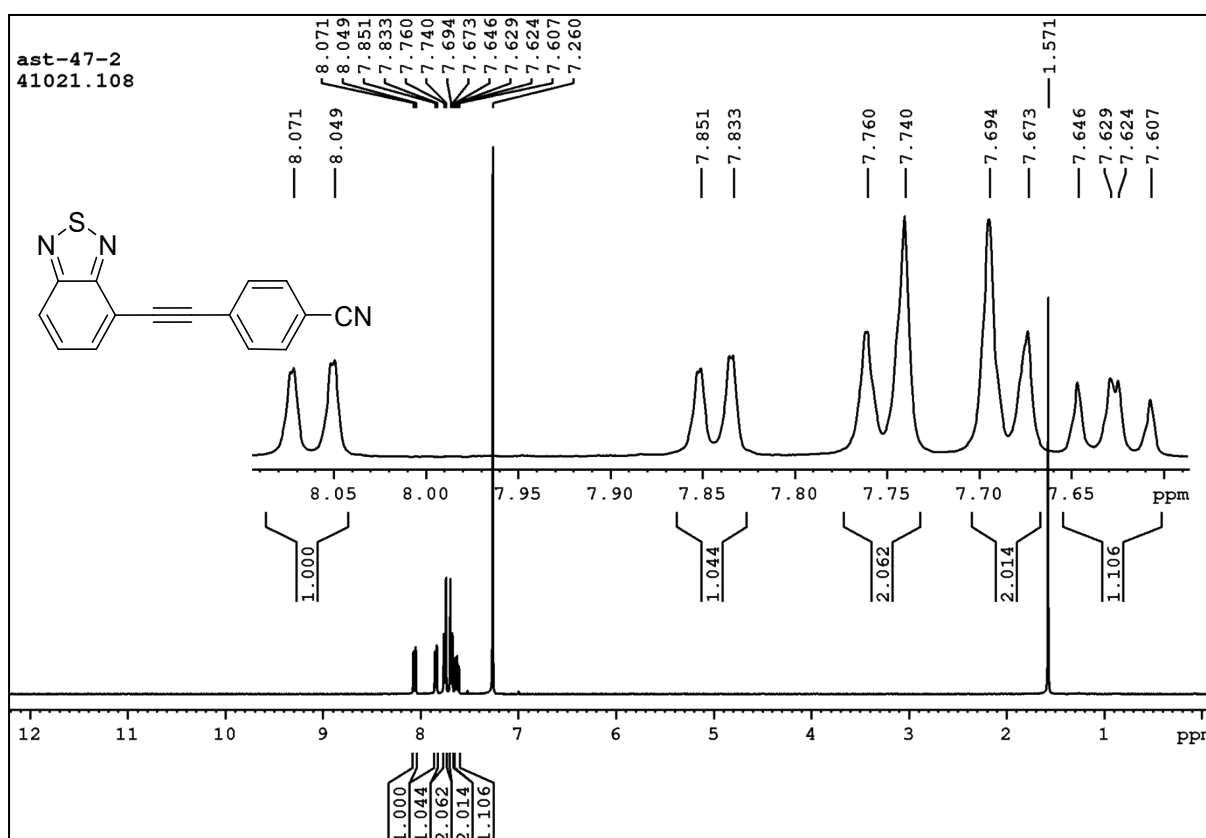
Fig. S3. ^{1}H NMR spectrum of **BTDPhCN** in CDCl$_3$.
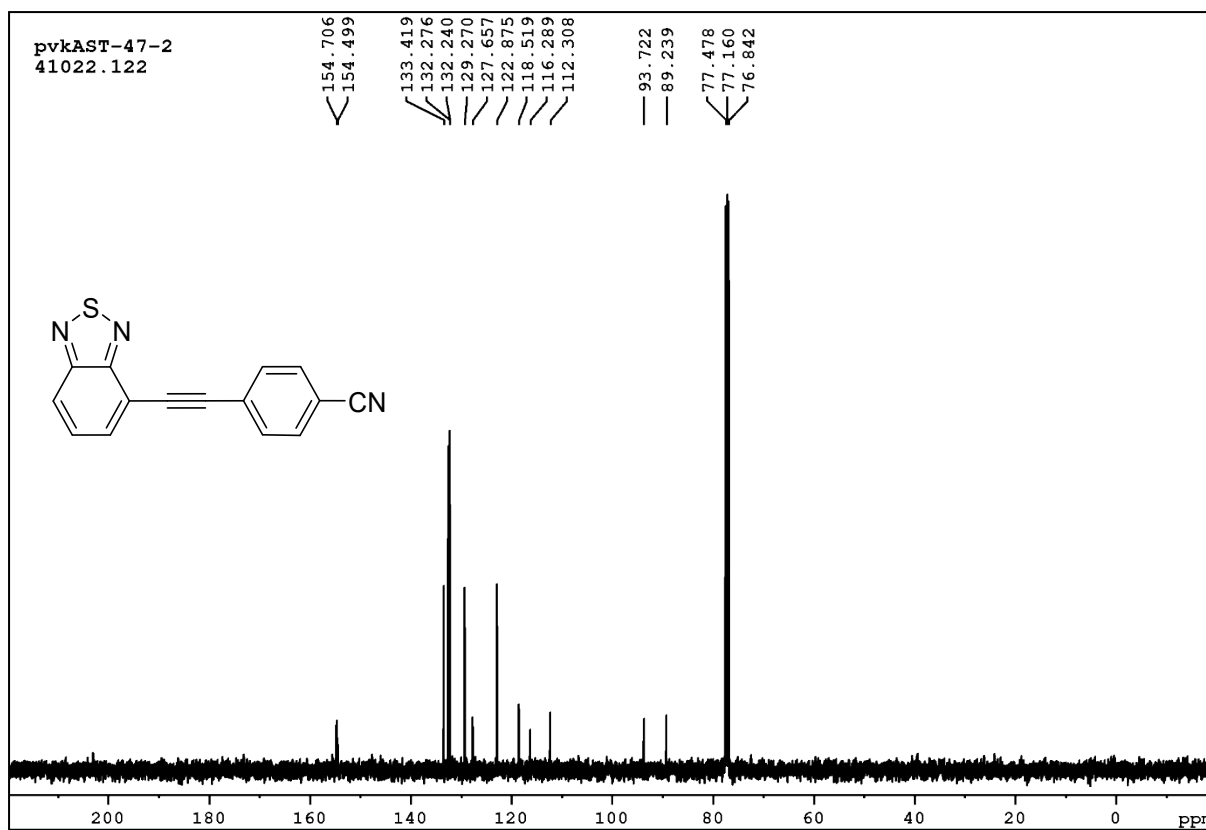
Fig. S4. ^{13}C NMR spectrum of **BTDPhCN** in CDCl$_3$.
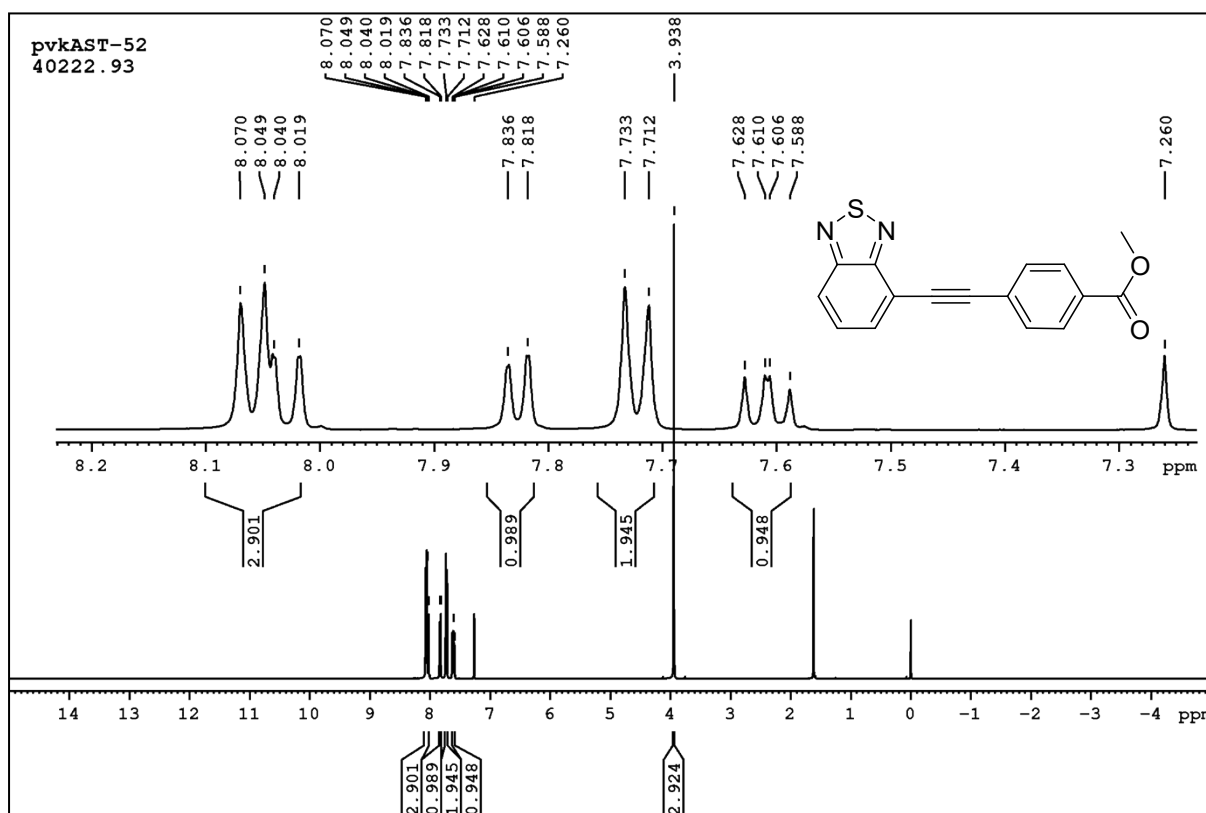
Fig. S5. ^{1}H NMR spectrum of **BTDPhCOOMe** in CDCl$_3$.
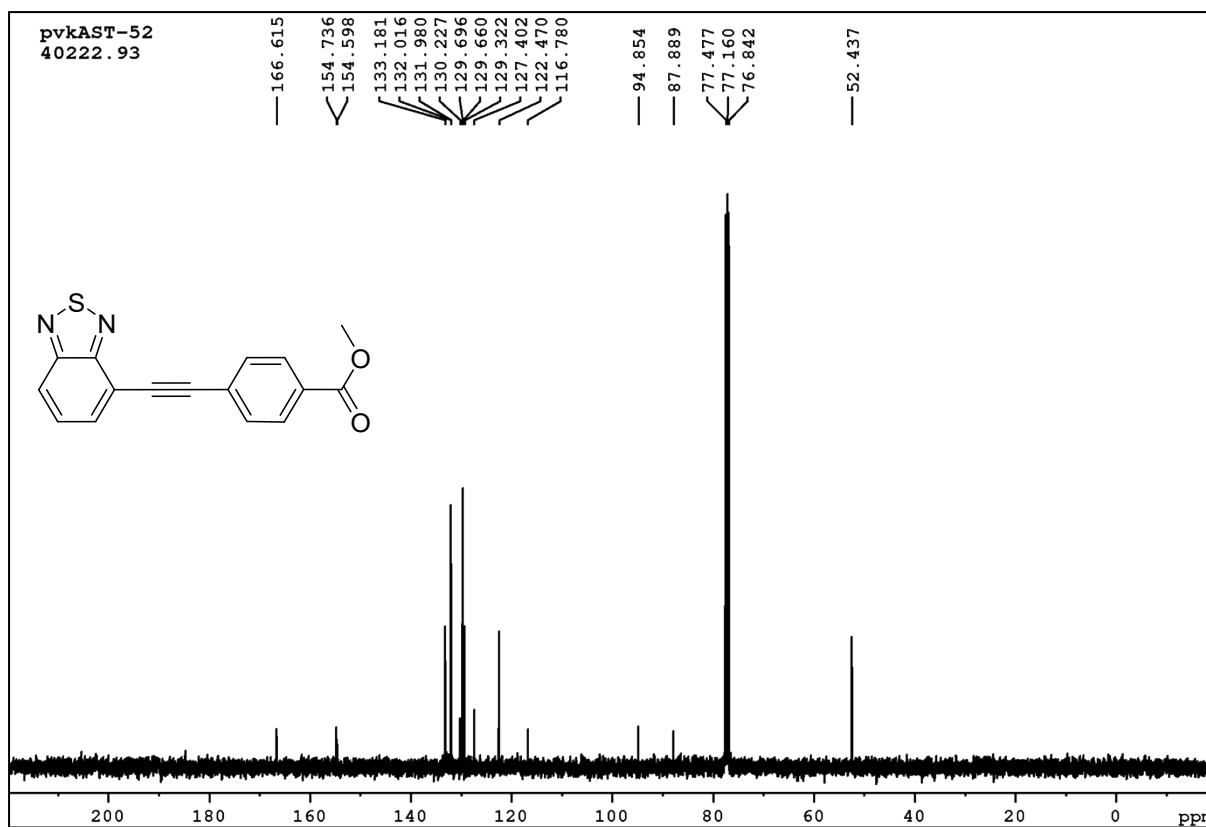
Fig. S6. ^{13}C NMR spectrum of **BTDPhCOOMe** in CDCl$_3$.
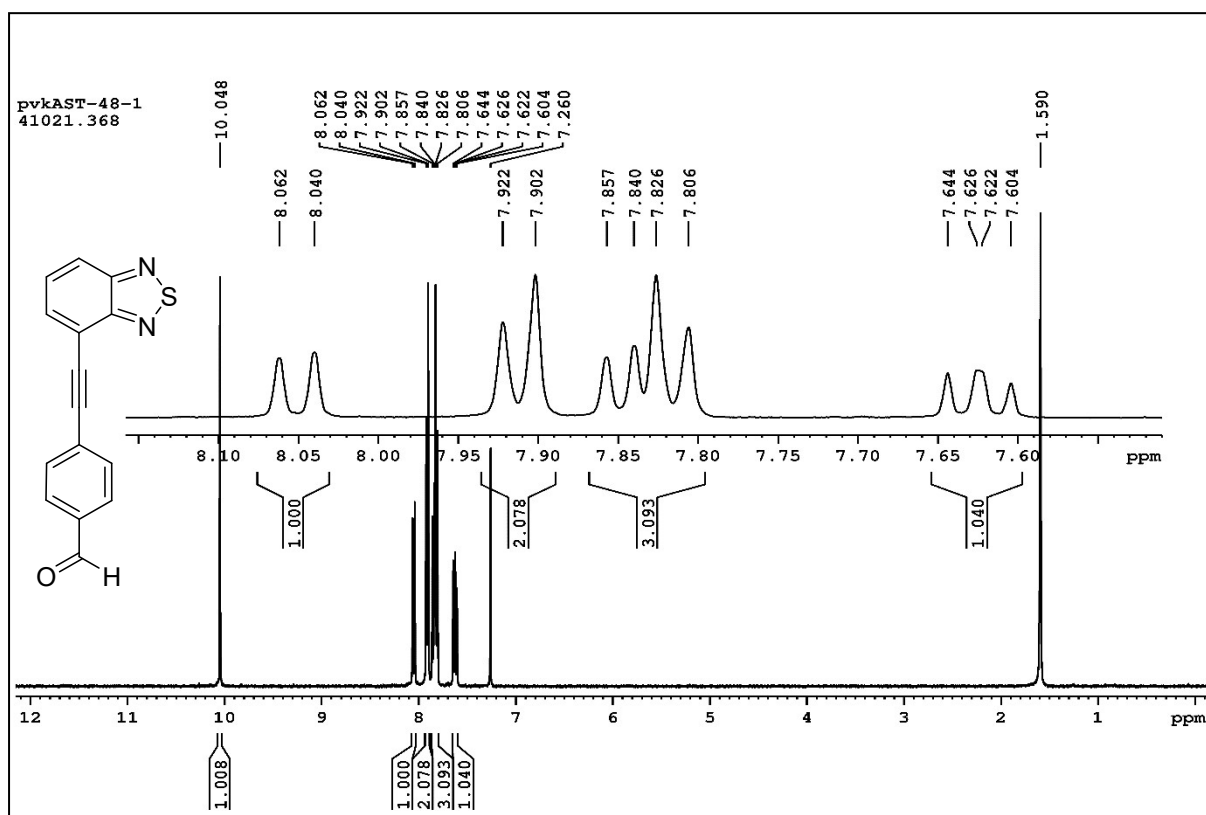
Fig. S7. ^{1}H NMR spectrum of **BTDPhCHO** in CDCl$_3$.
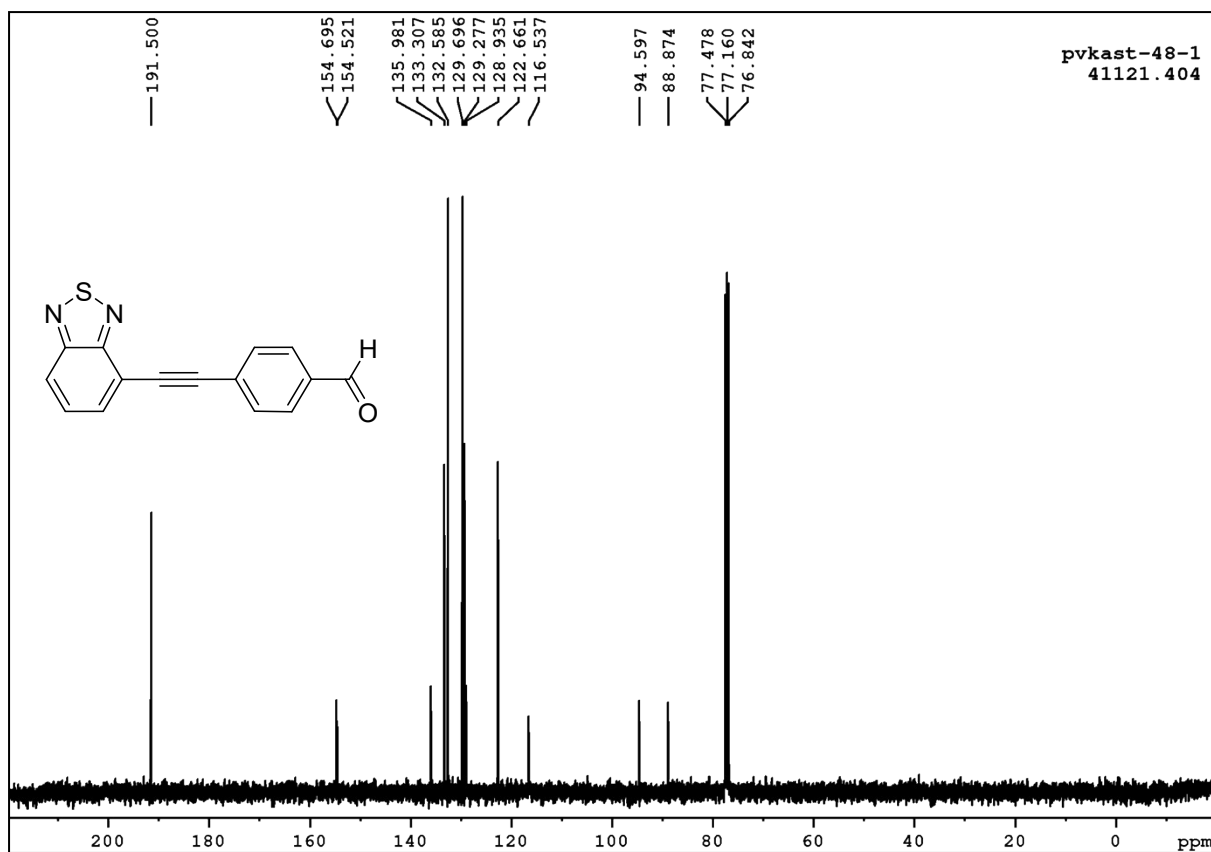
Fig. S8. ^{13}C NMR spectrum of **BTDPhCHO** in CDCl$_3$.

Fig. S9. ^{1}H NMR spectrum of **BTDPh** in CDCl$_3$.

pvkast-45
40821.233

154.729
154.681
132.750
132.079
129.326
129.033
128.509
128.737
122.737
121.869
117.314
95.896
85.172
77.478
77.160
76.842

200 180 160 140 120 100 80 60 40 20 0 ppm
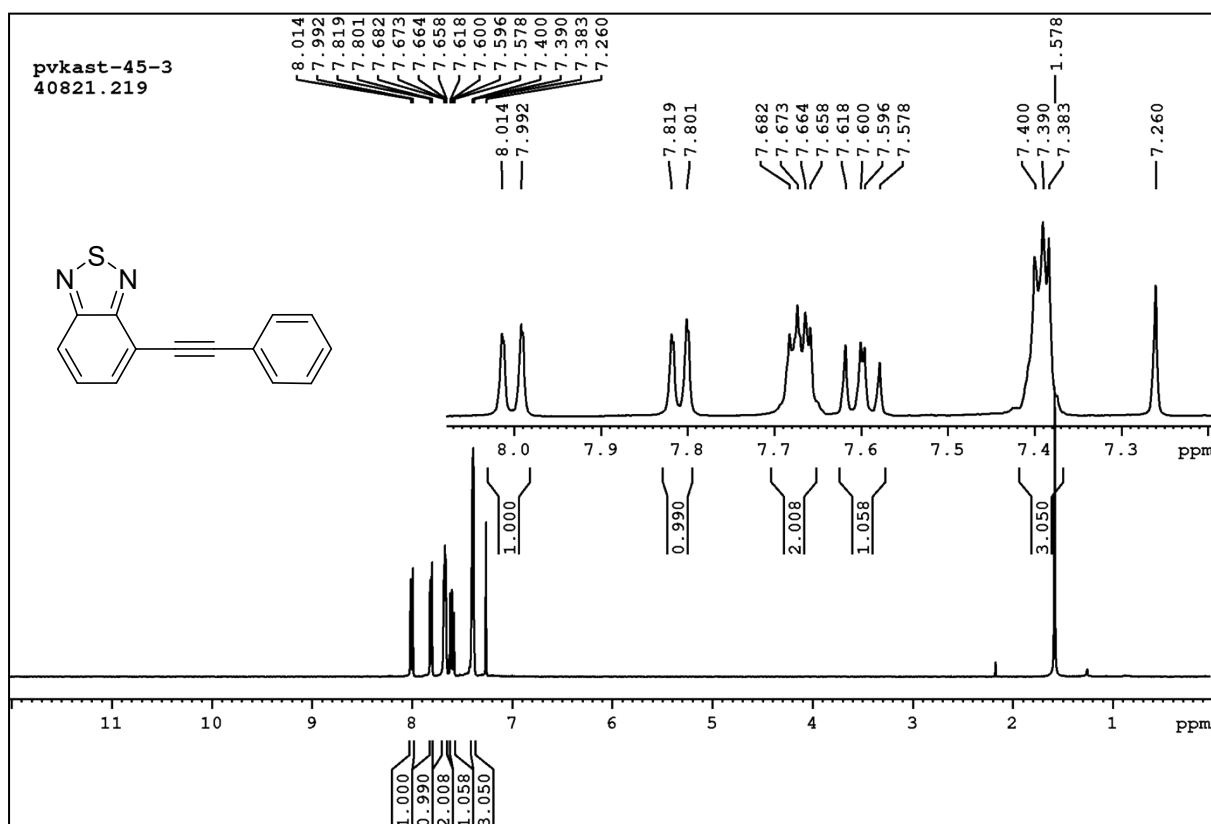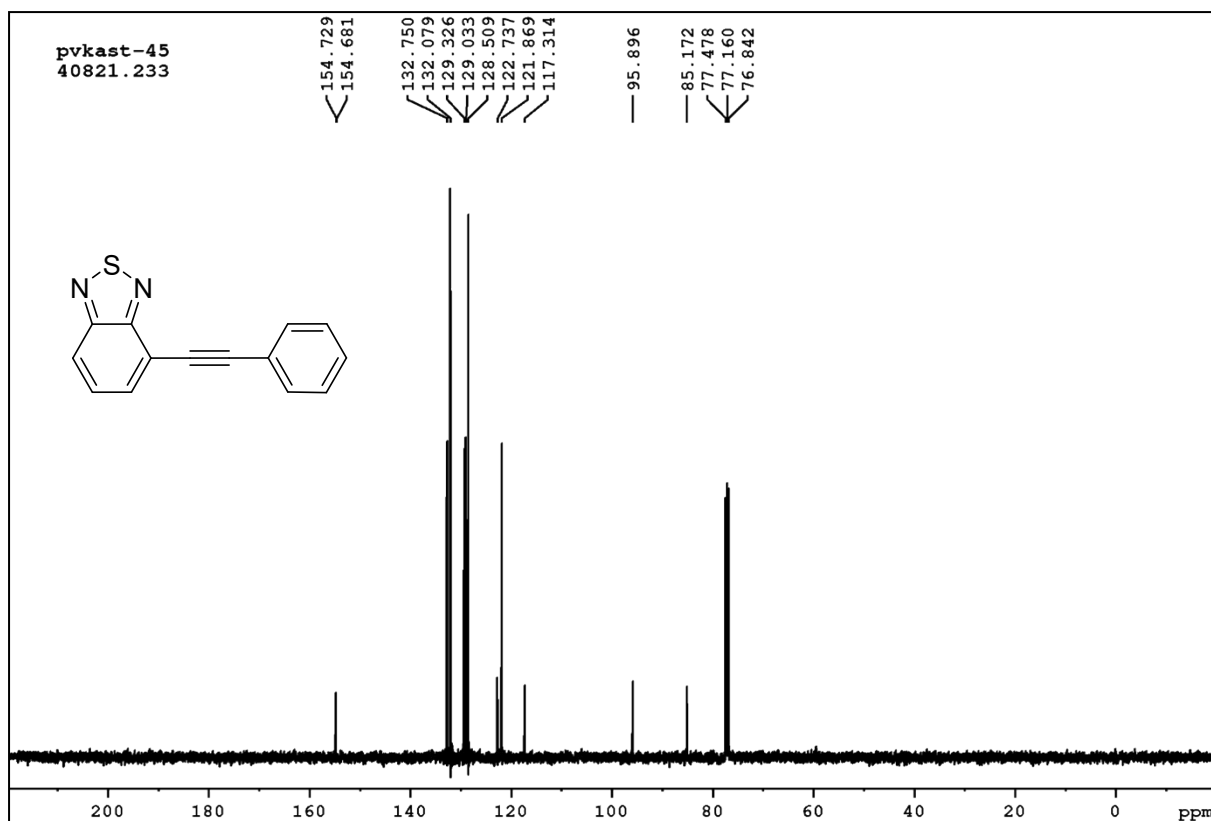
Fig. S10. ^{13}C NMR spectrum of **BTDPh** in CDCl$_3$.

pvkast-50-1
41221.28

8.021
7.999
7.835
7.818
7.753
7.733
7.647
7.626
7.613
7.609
7.591
7.485
7.467
7.447
7.395
7.377
7.359
7.260
1.577

8.021
7.999
7.835
7.818
7.753
7.733
7.647
7.626
7.613
7.609
7.591
7.485
7.467
7.447
7.395
7.377
7.359
7.260

8.0 7.9 7.8 7.7 7.6 7.5 7.4 ppm

1.028 1.065 2.046 5.079 2.039 1.007

12 11 10 9 8 7 6 5 4 3 2 1 ppm

1.028 1.065 2.046 5.079 2.039 1.007
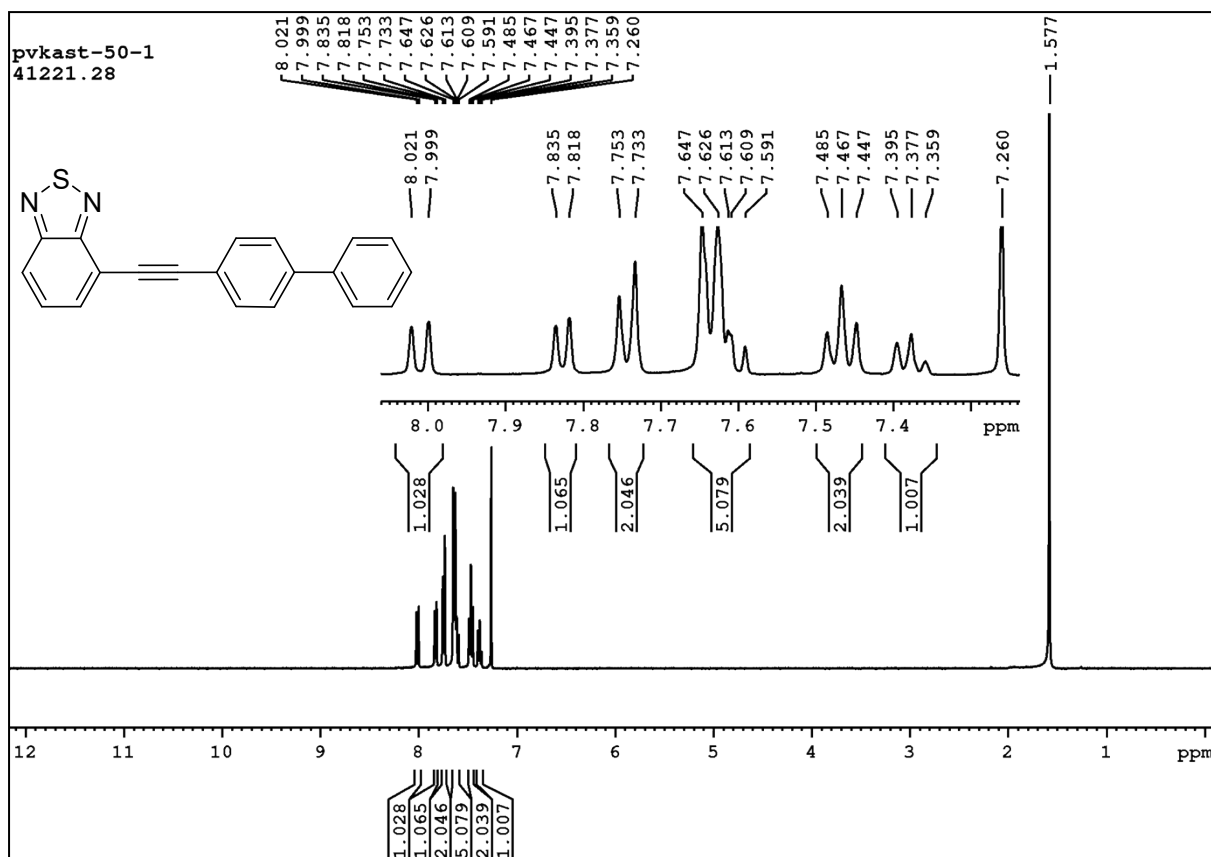
Fig. S11. ^{1}H NMR spectrum of **BTDPhPh** in CDCl$_3$.

14
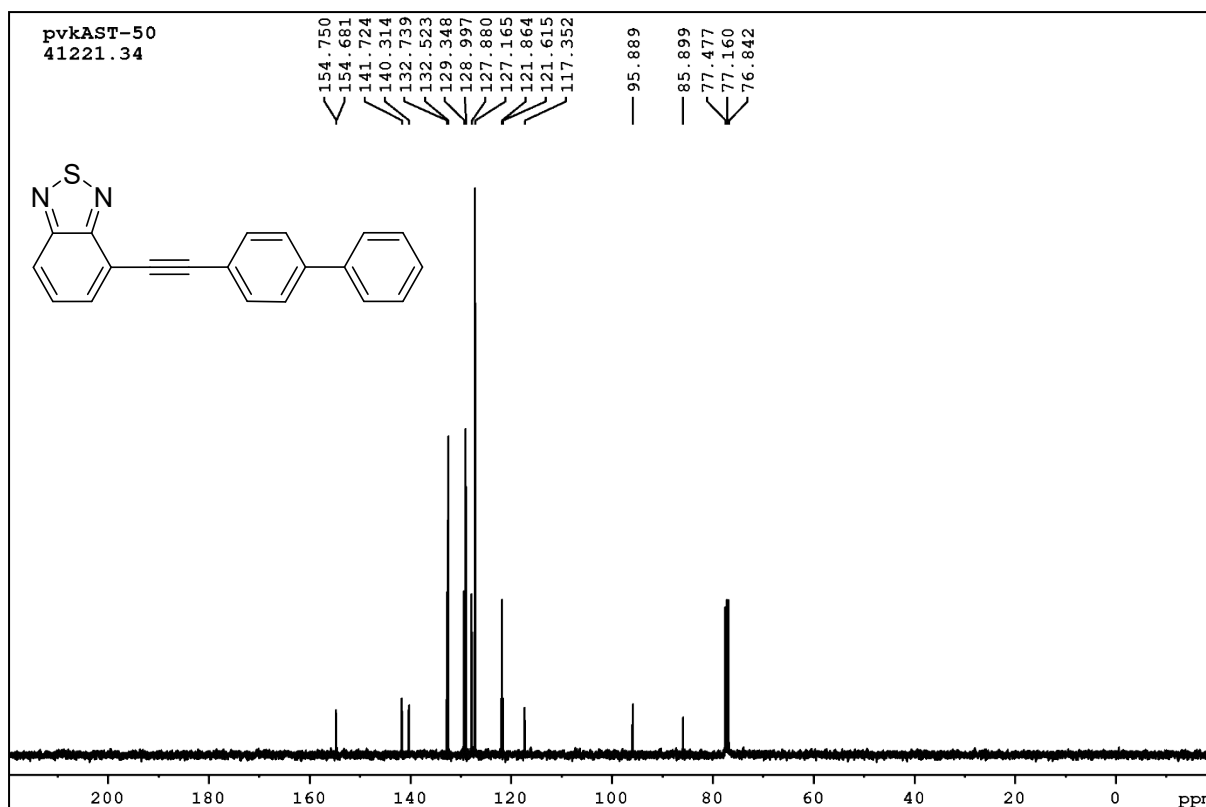
Fig. S12. ^{13}C NMR spectrum of **BTDPhPh** in CDCl$_3$.
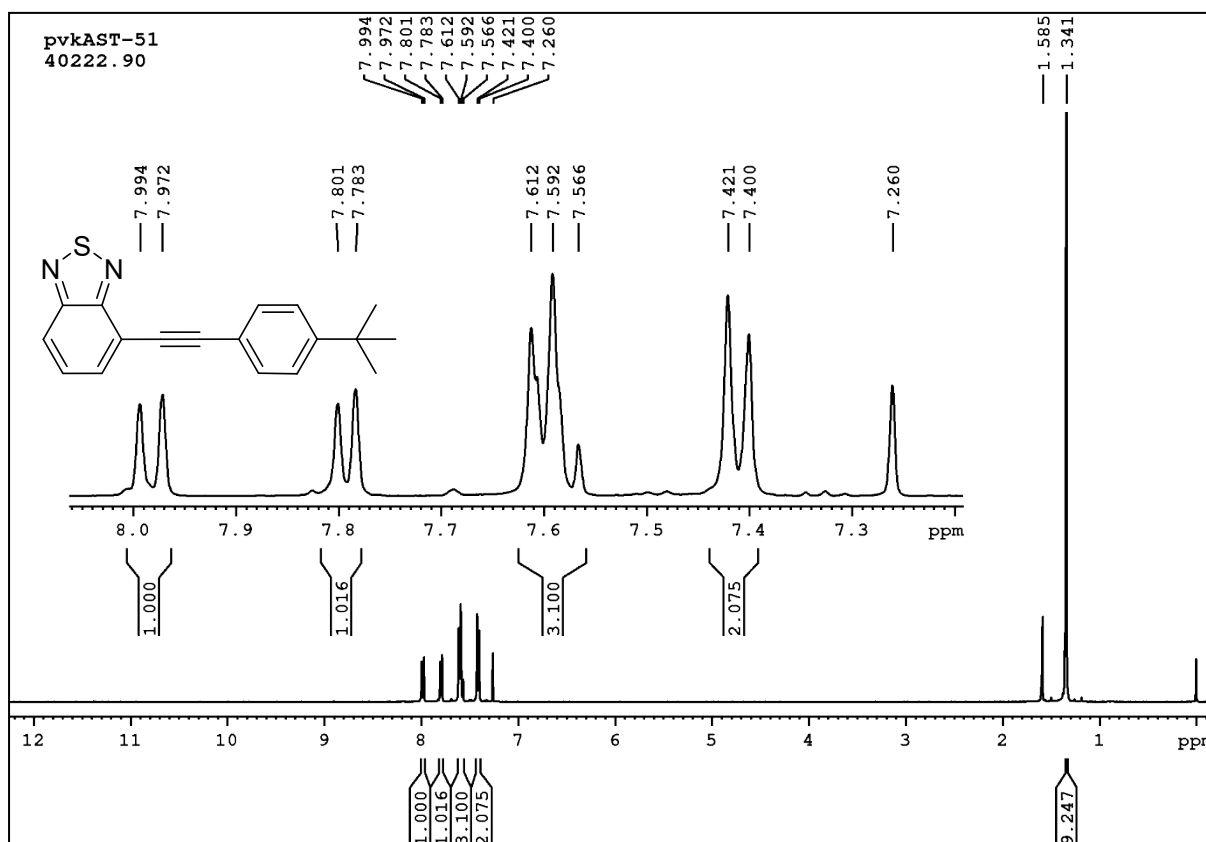
Fig. S13. ^1H NMR spectrum of **BTDPh^{t}But** in CDCl$_3$.
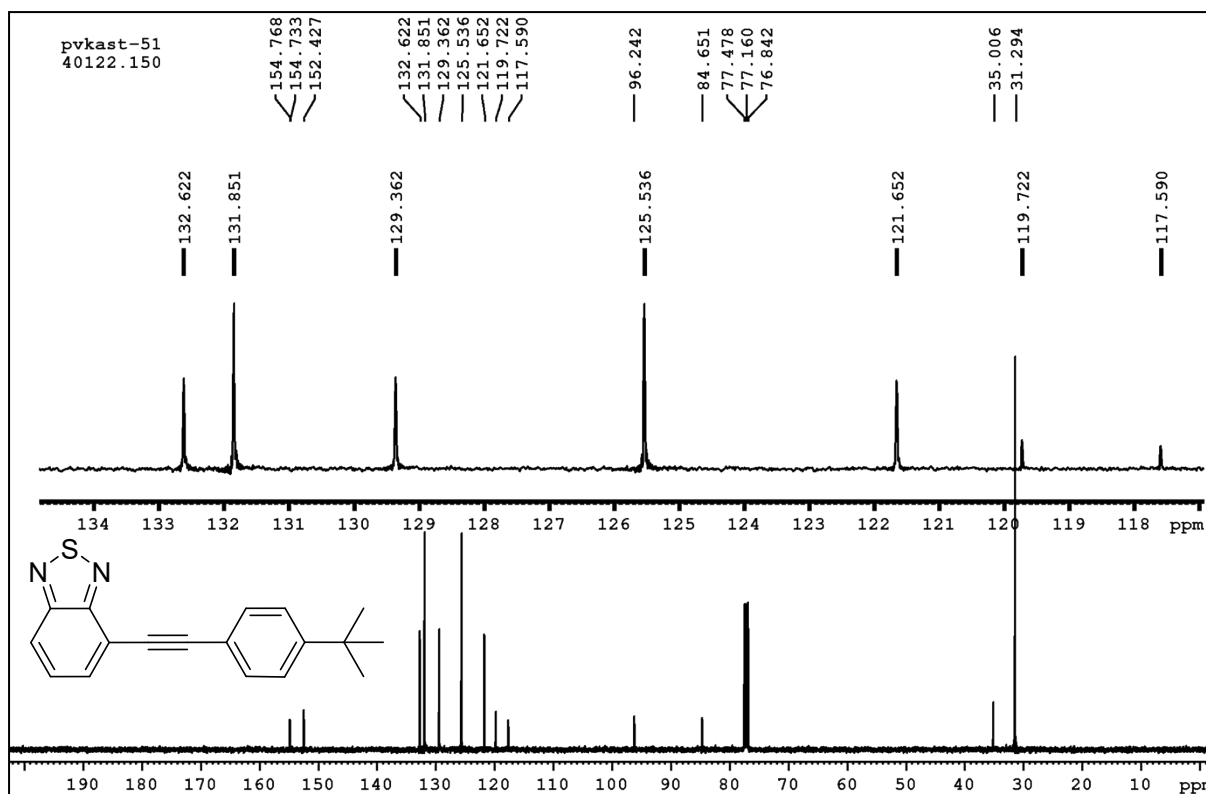
Fig. S14. ^{13}C NMR spectrum of **BTDPh^{t}But** in CDCl$_3$.

Fig. S15. ^{1}H NMR spectrum of **BTDPhOMe** in CDCl$_3$.

16

Fig. S16. ^{13}C NMR spectrum of **BTDPhOMe** in CDCl$_3$.
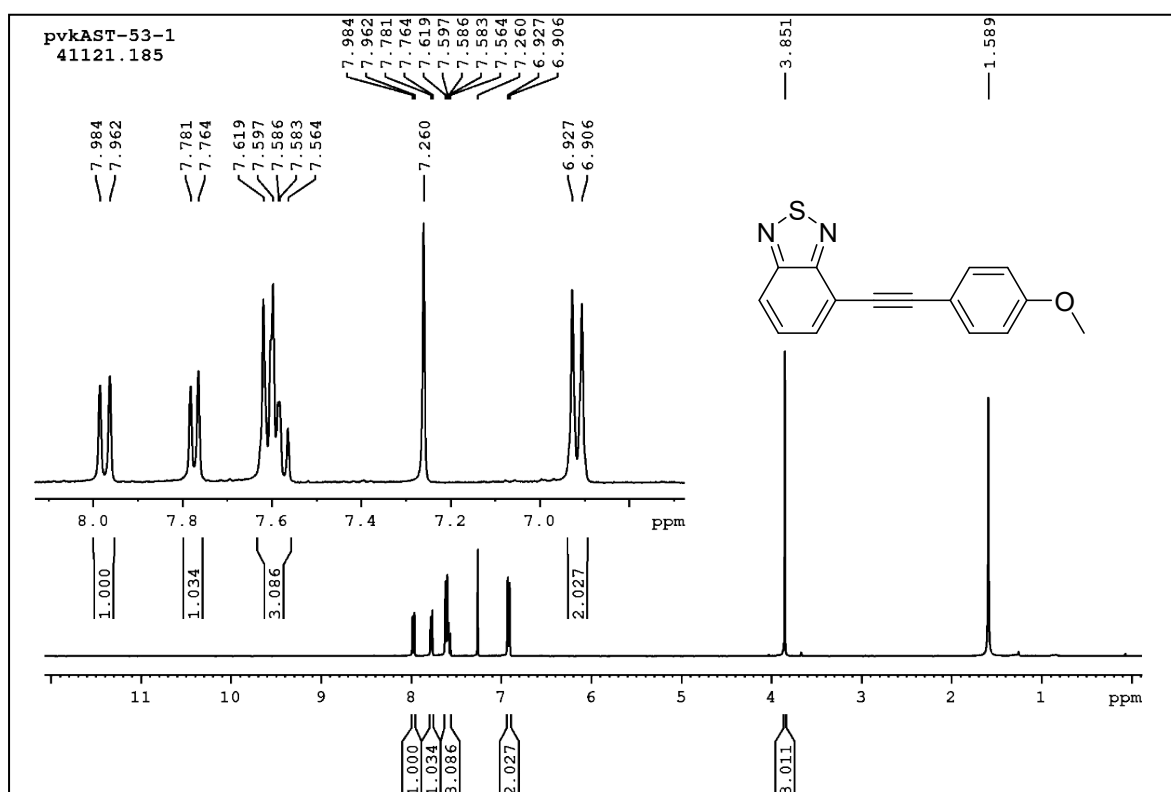
Fig. S17. ^{1}H NMR spectrum of **BTDPhNMe$_2$** in CDCl$_3$.
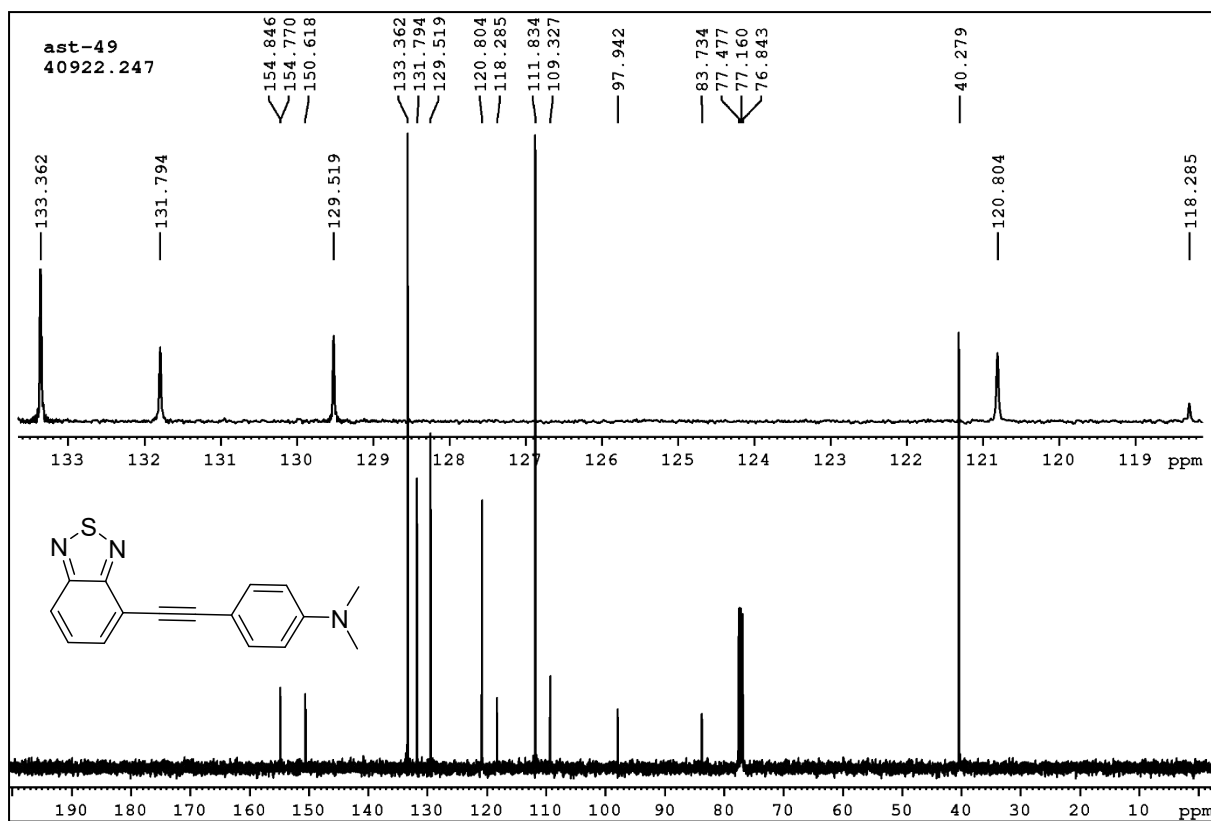
Fig. S18. ^{13}C NMR spectrum of **BTDPhNMe$_2$** in CDCl$_3$.

Table S1. Different substituents with their Hammett constant values (σ_p).

Substituents	Hammett constant value (σ_p)
Nitro (-NO$_2$)	0.78
Cyano(-CN)	0.66
Methoxy carbonyl (-COOMe)	0.45
Aldehyde (-CHO)	0.42
Hydrogen (-H)	0.00
Phenyl (-Ph)	-0.01
tert. Butyl (-^{t}But)	-0.20
Methoxy (-OMe)	-0.27
N,N-dimethyl amino (-NMe$_2$)	-0.83
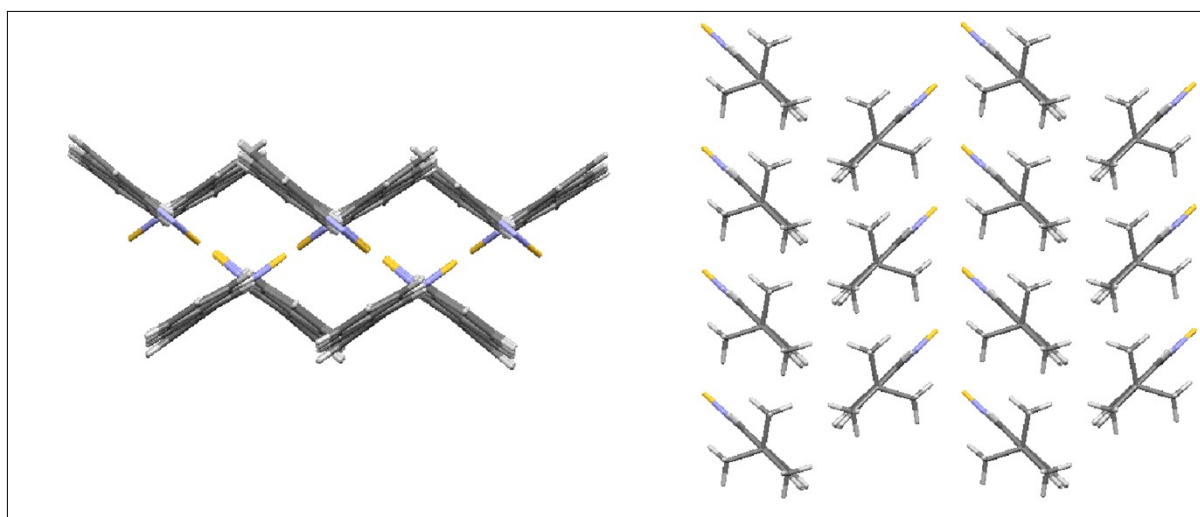
Fig. S19. The three-dimensional herringbone packing structure of (a)**BTDPhPh**, and (b) **BTDPhᵗBut**, respectively**.**

Table S2. Crystal data and structure refinement for **BTDPhPh**.

Identification code	50 (**CCDC: 2258215**)
Empirical formula	C20 H12 N2 S
Formula weight	312.38
Temperature	296(2) K
Wavelength	0.71073 Å
Crystal system	Monoclinic
Space group	P 21/c
Unit cell dimensions	$a = 11.3392(6)$ Å $\quad a= 90°$.
	$b = 5.6836(2)$ Å $\quad b= 93.381(2)°$
	$c = 24.2274(11)$ Å $\quad g = 90°$
Volume	1558.68(12) Å^3
Z	4
Density (calculated)	1.331 Mg/m^3
Absorption coefficient	0.208 mm^{-1}
F (000)	648
Crystal size	0.250 x 0.220 x 0.130 mm^3
Theta range for data collection	1.684 to 24.999°
Index ranges	-12<=h<=13, -6<=k<=4, -28<=l<=28
Reflections collected	10153
Independent reflections	2748 [R(int) = 0.0246]
Completeness to theta = 24.999°	100.0 %
Absorption correction	Semi-empirical from equivalents
Max. and min. transmission	0.974 and 0.950
Refinement method	Full-matrix least-squares on F^2
Data / restraints / parameters	2748 / 0 / 208
Goodness-of-fit on F^2	1.080

19

Final R indices [I>2sigma(I)]   R1 = 0.0498, wR2 = 0.1226
R indices (all data)   R1 = 0.0689, wR2 = 0.1432
Extinction coefficient   n/a

Largest diff. peak and hole   0.210 and -0.358 e.Å^{-3}

Bond lengths [Å] of **BTDPhPh**:

C(1)-C(6)	1.372(4)	C(12)-C(13)	1.375(3)
C(1)-C(2)	1.428(4)	C(12)-C(15)	1.487(3)
C(1)-H(1)	0.9300	C(13)-C(14)	1.382(3)
C(2)-C(3)	1.340(5)	C(13)-H(13)	0.9300
C(2)-H(2)	0.9300	C(14)-H(14)	0.9300
C(3)-C(4)	1.398(4)	C(15)-C(20)	1.379(3)
C(3)-H(3)	0.9300	C(15)-C(16)	1.380(3)
C(4)-N(1)	1.351(4)	C(16)-C(17)	1.389(3)
C(4)-C(5)	1.431(3)	C(16)-H(16)	0.9300
C(5)-N(2)	1.331(3)	C(17)-C(18)	1.350(4)
C(5)-C(6)	1.434(3)	C(17)-H(17)	0.9300
C(6)-C(7)	1.426(3)	C(18)-C(19)	1.360(4)
C(7)-C(8)	1.194(3)	C(18)-H(18)	0.9300
C(8)-C(9)	1.435(3)	C(19)-C(20)	1.384(3)
C(9)-C(14)	1.369(3)	C(19)-H(19)	0.9300
C(9)-C(10)	1.369(4)	C(20)-H(20)	0.9300
C(10)-C(11)	1.375(3)	N(1)-S(1)	1.601(3)
C(10)-H(10)	0.9300		
C(11)-C(12)	1.376(3)		
C(11)-H(11)	0.9300		
N(2)-S(1)	1.614(2)		

Bond angles [°] of **BTDPhPh**:

C(6)-C(1)-C(2)	121.4(3)	C(12)-C(13)-H(13)	118.7
C(6)-C(1)-H(1)	119.3	C(14)-C(13)-H(13)	118.7
C(2)-C(1)-H(1)	119.3	C(9)-C(14)-C(13)	120.9(2)
C(3)-C(2)-C(1)	122.4(3)	C(9)-C(14)-H(14)	119.6
C(3)-C(2)-H(2)	118.8	C(13)-C(14)-H(14)	119.6
C(1)-C(2)-H(2)	118.8	C(20)-C(15)-C(16)	116.7(2)
C(2)-C(3)-C(4)	118.7(3)	C(20)-C(15)-C(12)	121.4(2)
C(2)-C(3)-H(3)	120.6	C(16)-C(15)-C(12)	121.9(2)
C(4)-C(3)-H(3)	120.6	C(15)-C(16)-C(17)	121.4(2)
N(1)-C(4)-C(3)	127.7(2)	C(15)-C(16)-H(16)	119.3
N(1)-C(4)-C(5)	112.0(3)	C(17)-C(16)-H(16)	119.3
C(3)-C(4)-C(5)	120.3(3)	C(18)-C(17)-C(16)	120.7(2)
N(2)-C(5)-C(4)	113.8(2)	C(18)-C(17)-H(17)	119.7
N(2)-C(5)-C(6)	125.9(2)	C(16)-C(17)-H(17)	119.7
C(4)-C(5)-C(6)	120.3(2)	C(17)-C(18)-C(19)	119.0(2)
C(1)-C(6)-C(7)	123.2(2)	C(17)-C(18)-H(18)	120.5
C(1)-C(6)-C(5)	116.9(2)	C(19)-C(18)-H(18)	120.5
C(7)-C(6)-C(5)	119.9(2)	C(18)-C(19)-C(20)	120.9(3)
C(8)-C(7)-C(6)	179.3(3)	C(18)-C(19)-H(19)	119.6
C(7)-C(8)-C(9)	178.2(3)	C(20)-C(19)-H(19)	119.6
C(14)-C(9)-C(10)	117.1(2)	C(15)-C(20)-C(19)	121.3(2)
C(14)-C(9)-C(8)	120.7(2)	C(15)-C(20)-H(20)	119.4

C(10)-C(9)-C(8)	122.2(2)	C(19)-C(20)-H(20)	119.4
C(9)-C(10)-C(11)	121.7(2)	C(4)-N(1)-S(1)	107.00(17)
C(9)-C(10)-H(10)	119.1	C(5)-N(2)-S(1)	106.44(16)
C(11)-C(10)-H(10)	119.1	N(1)-S(1)-N(2)	100.71(13)
C(12)-C(11)-C(10)	122.1(2)		
C(12)-C(11)-H(11)	119.0		
C(10)-C(11)-H(11)	119.0		
C(13)-C(12)-C(11)	115.7(2)		
C(13)-C(12)-C(15)	122.2(2)		
C(11)-C(12)-C(15)	122.2(2)		
C(12)-C(13)-C(14)	122.6(2)		

Table S3. Crystal data and structure refinement for **BTDPh^{t}But**.

|	
Identification code	511 (**CCDC: 2260324**)
Empirical formula	C18 H16 N2 S
Formula weight	292.39
Temperature	296(2) K
Wavelength	0.71073 Å
Crystal system	Monoclinic
Space group	P 21/c
Unit cell dimensions	a = 18.867(5) Å a= 90°.
	b = 10.278(3) Å b= 92.057(11)°
	c = 8.239(2) Å g = 90°
Volume	1596.6(7) Å^3
Z	4
Density (calculated)	1.216 Mg/m^3
Absorption coefficient	0.197 mm^{-1}
F (000)	616
Crystal size	0.150 x 0.120 x 0.100 mm^3
Theta range for data collection	2.160 to 24.421°
Index ranges	-21<=h<=21, -11<=k<=11, -9<=l<=8
Reflections collected	10898
Completeness to theta = 24.421°	98.6 %
Absorption correction	None
Refinement method	Full-matrix least-squares on F^2
Data / restraints / parameters	10898 / 0 / 226
Goodness-of-fit on F^2	1.162
Final R indices [I>2sigma(I)]	R1 = 0.1005, wR2 = 0.2729
R indices (all data)	R1 = 0.1407, wR2 = 0.2919
Extinction coefficient	0.004(2)
Largest diff. peak and hole	0.449 and -0.498 e.Å^{-3}

Bond lengths [Å] of **BTDPh^{t}But**:

C(1)-C(6)	1.384(11)	C(15)-C(18)	1.54(2)
C(1)-C(2)	1.412(14)	C(15)-C(17)	1.57(2)

C(1)-H(1)	0.9300	C(15)-C(17A)	1.57(3)
C(2)-C(3)	1.340(14)	C(16)-H(16A)	0.9600
C(2)-H(2)	0.9300	C(16)-H(16B)	0.9600
C(3)-C(4)	1.423(12)	C(16)-H(16C)	0.9600
C(3)-H(3)	0.9300	C(17)-H(17A)	0.9600
C(4)-N(1)	1.332(10)	C(17)-H(17B)	0.9600
C(4)-C(5)	1.409(12)	C(17)-H(17C)	0.9600
C(5)-N(2)	1.347(9)	C(18)-H(18A)	0.9600
C(5)-C(6)	1.415(11)	C(18)-H(18B)	0.9600
C(6)-C(7)	1.415(13)	C(18)-H(18C)	0.9600
C(7)-C(8)	1.190(13)	C(17A)-H(17D)	0.9600
C(8)-C(9)	1.438(13)	C(17A)-H(17E)	0.9600
C(9)-C(14)	1.364(12)	C(17A)-H(17F)	0.9600
C(9)-C(10)	1.393(11)	C(16A)-H(16D)	0.9600
C(10)-C(11)	1.370(13)	C(16A)-H(16E)	0.9600
C(10)-H(10)	0.9300	C(16A)-H(16F)	0.9600
C(11)-C(12)	1.396(12)	C(18A)-H(18D)	0.9600
C(11)-H(11)	0.9300	C(18A)-H(18E)	0.9600
C(12)-C(13)	1.378(11)	C(18A)-H(18F)	0.9600
C(12)-C(15)	1.528(13)	N(1)-S(1)	1.620(9)
C(13)-C(14)	1.396(13)	N(2)-S(1)	1.598(8)
C(13)-H(13)	0.9300		
C(14)-H(14)	0.9300		
C(15)-C(16A)	1.46(3)		
C(15)-C(16)	1.506(18)		
C(15)-C(18A)	1.52(3)		

Bond angle [°] of **BTDPh^{t}But**:

|			
C(6)-C(1)-C(2)	122.6(9)	C(12)-C(15)-C(17A)	105.2(14)
C(6)-C(1)-H(1)	118.7	C(15)-C(16)-H(16A)	109.5
C(2)-C(1)-H(1)	118.7	C(15)-C(16)-H(16B)	109.5
C(3)-C(2)-C(1)	122.5(9)	H(16A)-C(16)-H(16B)	109.5
C(3)-C(2)-H(2)	118.8	C(15)-C(16)-H(16C)	109.5
C(1)-C(2)-H(2)	118.8	H(16A)-C(16)-H(16C)	109.5
C(2)-C(3)-C(4)	117.7(10)	H(16B)-C(16)-H(16C)	109.5
C(2)-C(3)-H(3)	121.2	C(15)-C(17)-H(17A)	109.5
C(4)-C(3)-H(3)	121.2	C(15)-C(17)-H(17B)	109.5
N(1)-C(4)-C(5)	114.4(8)	H(17A)-C(17)-H(17B)	109.5
N(1)-C(4)-C(3)	125.8(10)	C(15)-C(17)-H(17C)	109.5
C(5)-C(4)-C(3)	119.7(9)	H(17A)-C(17)-H(17C)	109.5
N(2)-C(5)-C(4)	112.7(8)	H(17B)-C(17)-H(17C)	109.5
N(2)-C(5)-C(6)	124.8(8)	C(15)-C(18)-H(18A)	109.5
C(4)-C(5)-C(6)	122.5(8)	C(15)-C(18)-H(18B)	109.5
C(1)-C(6)-C(5)	115.0(9)	H(18A)-C(18)-H(18B)	109.5
C(1)-C(6)-C(7)	122.3(9)	C(15)-C(18)-H(18C)	109.5
C(5)-C(6)-C(7)	122.6(7)	H(18A)-C(18)-H(18C)	109.5
C(8)-C(7)-C(6)	179.6(11)	H(18B)-C(18)-H(18C)	109.5
C(7)-C(8)-C(9)	178.8(10)	C(15)-C(17A)-H(17D)	109.5
C(14)-C(9)-C(10)	117.8(9)	C(15)-C(17A)-H(17E)	109.5
C(14)-C(9)-C(8)	122.0(8)	H(17D)-C(17A)-H(17E)	109.5
C(10)-C(9)-C(8)	120.2(9)	C(15)-C(17A)-H(17F)	109.5
C(11)-C(10)-C(9)	121.3(9)	H(17D)-C(17A)-H(17F)	109.5
C(11)-C(10)-H(10)	119.4	H(17E)-C(17A)-H(17F)	109.5
C(9)-C(10)-H(10)	119.4	C(15)-C(16A)-H(16D)	109.5
C(10)-C(11)-C(12)	121.5(9)	C(15)-C(16A)-H(16E)	109.5
C(10)-C(11)-H(11)	119.3	H(16D)-C(16A)-H(16E)	109.5

C(12)-C(11)-H(11)	119.3	C(15)-C(16A)-H(16F)	109.5
C(13)-C(12)-C(11)	116.8(9)	H(16D)-C(16A)-H(16F)	109.5
C(13)-C(12)-C(15)	122.0(8)	H(16E)-C(16A)-H(16F)	109.5
C(11)-C(12)-C(15)	121.2(8)	C(15)-C(18A)-H(18D)	109.5
C(12)-C(13)-C(14)	121.6(9)	C(15)-C(18A)-H(18E)	109.5
C(12)-C(13)-H(13)	119.2	H(18D)-C(18A)-H(18E)	109.5
C(14)-C(13)-H(13)	119.2	C(15)-C(18A)-H(18F)	109.5
C(9)-C(14)-C(13)	121.0(8)	H(18D)-C(18A)-H(18F)	109.5
C(9)-C(14)-H(14)	119.5	H(18E)-C(18A)-H(18F)	109.5
C(13)-C(14)-H(14)	119.5	C(4)-N(1)-S(1)	105.5(7)
C(16A)-C(15)-C(18A)	110(2)	C(5)-N(2)-S(1)	106.5(6)
C(16A)-C(15)-C(12)	112.3(13)	N(2)-S(1)-N(1)	100.8(4)
C(16)-C(15)-C(12)	111.6(11)		
C(18A)-C(15)-C(12)	112.6(15)		
C(16)-C(15)-C(18)	108.8(16)		
C(12)-C(15)-C(18)	114.1(11)		
C(16)-C(15)-C(17)	109.9(15)		
C(12)-C(15)-C(17)	106.8(10)		
C(18)-C(15)-C(17)	105.4(15)		
C(16A)-C(15)-C(17A)	109(2)		
C(18A)-C(15)-C(17A)	107(2)		
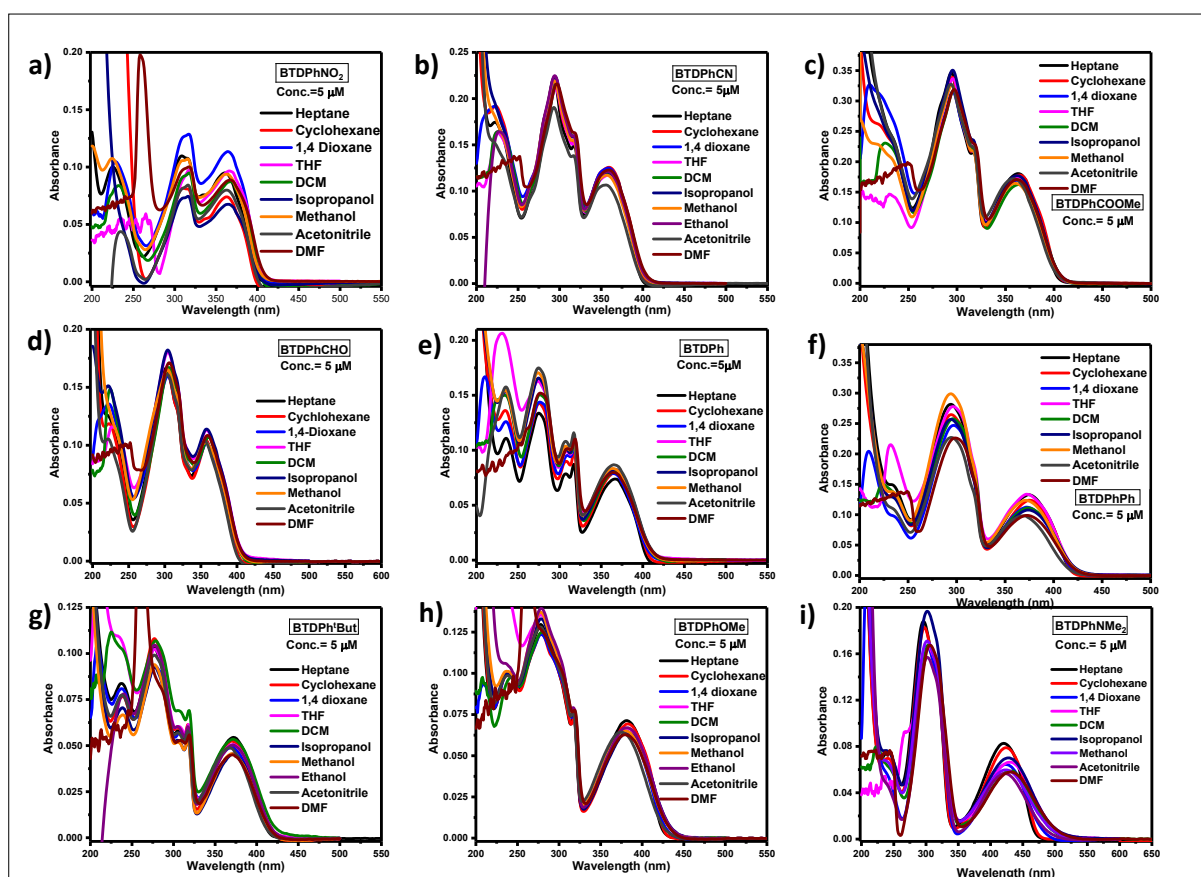
Fig. S20. Steady-state absorption spectra of (a) **BTDPhNO₂**, (b) **BTDPhCN**, (c) **BTDPhCOOMe**, (d) **BTDPhCHO**, (e) **BTDPh** and (f) **BTDPhPh,** (g) **BTDPhᵗBut**, (h) **BTDPhOMe**, (i) **BTDPhNMe₂** in solvents of different polarities. ([**BTDs**] = 5 x 10⁻⁶ M)
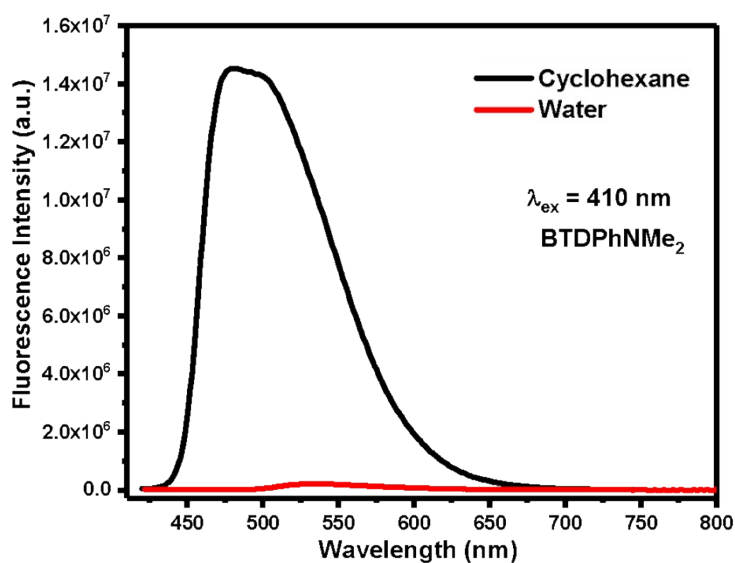
Fig. S21. Shows the emission spectra (λ_{ex} = 410 nm) of **BTDPhNMe₂** in cyclohexane and water (5 x 10⁻⁶ M).
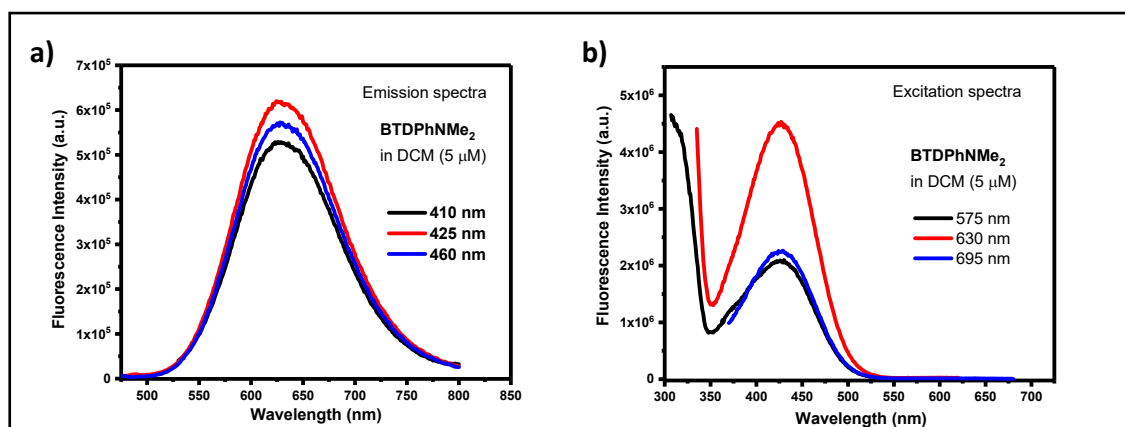
Fig. S22. Shows the (a) emission spectra, and (b) excitation spectra of **BTDPhNMe₂** in DCM, respectively (5 x 10⁻⁶ M).

Table S4. Absorption, emission parameters, Stokes shifts and quantum yields of **BTDPhNO₂**, **BTDPhCN**, and **BTDPhCOOMe** in solvents of varying polarities ((ε-1)/(ε+2)). Where ε is the dielectric constant of respective solvent medium.
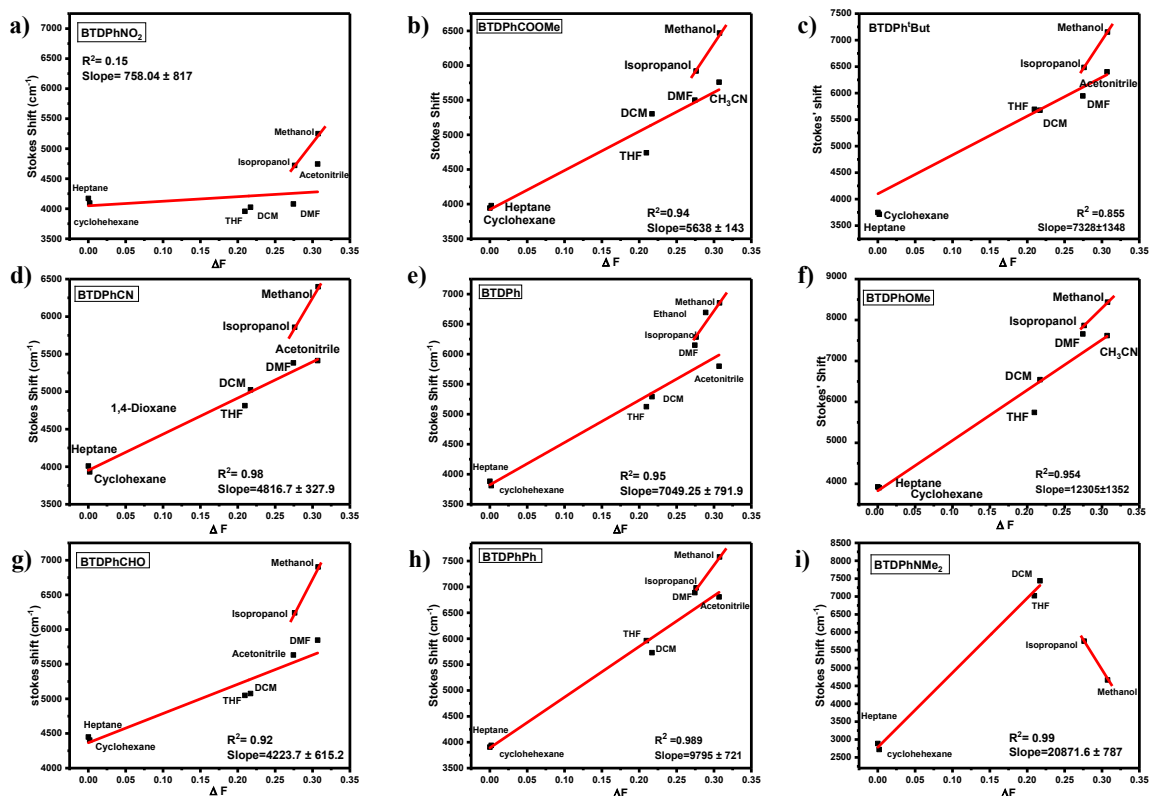
Solvents	$\dfrac{(\varepsilon - 1)}{(\varepsilon + 2)}$	BTDPhNO₂			BTDPhCN				BTDPhCOOMe			
		λ_{abs} (nm)	λ_{em} (nm)	Stokes shift (cm⁻¹)	λ_{abs} (nm)	λ_{em} (nm)	Stokes shift (cm⁻¹)	Q.Y. (ϕ_f)	λ_{abs} (nm)	λ_{em} (nm)	Stokes shift (cm⁻¹)	Q.Y. (ϕ_f)
n-Heptane	0.235	361	425	4171	358	418	4010	--	364	425	3943	--
Cyclohexane	0.254	362	425	4095	359	418	3932	0.28	365	427	3978	0.28
1,4-Dioxane	0.294	364	427	4053	359	432	4707	0.29	362	439	4845	0.37
THF	0.687	366	428	3958	359	434	4814	0030	362	437	4741	0.29
DCM	0.726	368	432	4026	359	438	5024	0.25	362	448	5303	0.35
2-Propanol	0.863	365	441	4722	358	453	5858	0.36	364	464	5921	0.49

Methanol	0.914	364	450	5250	356	461	6398	0.40	361	471	6469	0.52
DMF	0.922	368	433	4079	359	445	5383	0.38	362	452	5500	0.43
ACN	0.924	364	440	4745	356	441	5414	0.31	358	451	5760	0.41

Table S5. Absorption, emission parameters, Stokes shifts and quantum yields of **BTDPhCHO**, **BTDPh** and **BTDPhPh** in solvents of varying polarities ($(\varepsilon-1)/(\varepsilon+2)$). Where ε is the dielectric constant of respective solvent medium.

Solvents	$\dfrac{(\varepsilon-1)}{(\varepsilon+2)}$	BTDPhCHO				BTDPh				BTDPhPh			
		λ_{abs} (nm)	λ_{em} (nm)	Stokes shift (cm^{-1})	Q.Y. (ϕ_f)	λ_{abs} (nm)	λ_{em} (nm)	Stokes shift (cm^{-1})	Q.Y. (ϕ_f)	λ_{abs} (nm)	λ_{em} (nm)	Stokes shift (cm^{-1})	Q.Y. (ϕ_f)
n-Heptane	0.235	356	423	4449	--	367	428	3883	--	374	438	3907	--
Cyclohexane	0.254	358	425	4404	0.08	368	428	3809	0.40	375	440	3939	0.43
1,4-Dioxane	0.294	358	437	5050	0.13	364	445	5001	0.74	374	462	5093	0.49
THF	0.687	358	437	5050	0.14	365	449	5126	0.66	375	483	5963	0.46
DCM	0.726	361	442	5076	0.20	368	457	5292	0.82	374	476	5730	0.64
2-Propanol	0.863	358	461	6241	0.22	367	477	6284	0.81	373	492	6484	0.56
Methanol	0.914	356	472	6903	0.29	364	485	6854	0.44	373	520	7579	0.27
DMF	0.922	359	450	5633	0.23	361	464	6149	0.71	373	502	6889	0.57
ACN	0.924	355	448	5848	0.28	365	463	5799	0.67	368	491	6807	0.64

Table S6. Absorption, emission parameters, Stokes shifts and quantum yields of **BTDPhᵗBut**, **BTDPhOMe** and **BTDPhNMe₂** in solvents of varying polarities ($(\varepsilon-1)/(\varepsilon+2)$). Where ε is the dielectric constant of respective solvent medium.

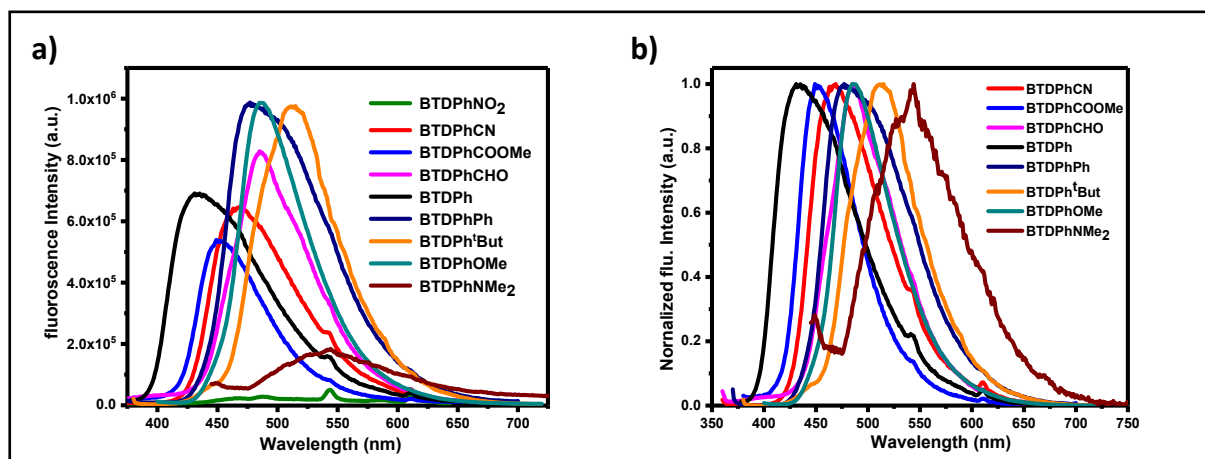| Solvents	$\dfrac{(\varepsilon-1)}{(\varepsilon+2)}$	BTDPhᵗBut				BTDPhOMe				BTDPhNMe₂			
		λ_{abs} (nm)	λ_{em} (nm)	Stokes shift (cm^{-1})	Q.Y. (ϕ_f)	λ_{abs} (nm)	λ_{em} (nm)	Stokes shift (cm^{-1})	Q.Y. (ϕ_f)	λ_{abs} (nm)	λ_{em} (nm)	Stokes shift (cm^{-1})	Q.Y. (ϕ_f)
n-Heptane	0.235	374	435	3749	--	381	448	3925	--	420	478	2889	--
Cyclohexane	0.254	373	433	3715	0.56	382	449	3906	0.87	423	478	2720	0.66
1,4-Dioxane	0.294	370	456	5097	0.80	378	476	5447	0.80	423	578	6340	0.24
THF	0.687	372	472	5695	0.77	383	491	5743	0.79	430	616	7022	< 0.05
DCM	0.726	371	470	5678	0.88	379	504	6544	0.69	428	628	7441	< 0.05
2-Propanol	0.863	373	492	6484	0.67	379	540	7867	0.18	427	566	5751	--
Methanol	0.914	371	505	7152	0.56	378	555	8437	0.23	423	527	4665	--
DMF	0.922	374	481	5948	0.90	380	536	7659	0.32	431	--	--	--
ACN	0.924	366	478	6402	0.84	375	525	7619	0.60	421	--	--	--
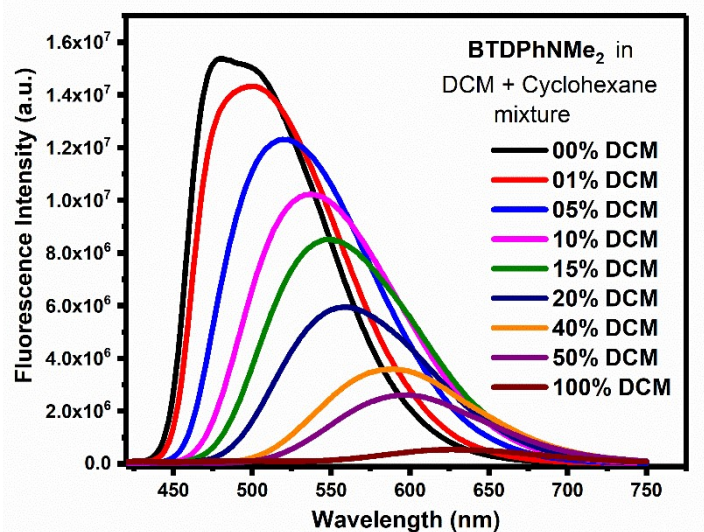
Fig. S23. Fluorescence emission spectra (λ_{ex} = 410 nm) of **BTDPhNMe$_2$** in different fraction of DCM in cyclohexane solution (5 x 10^{-6} M).
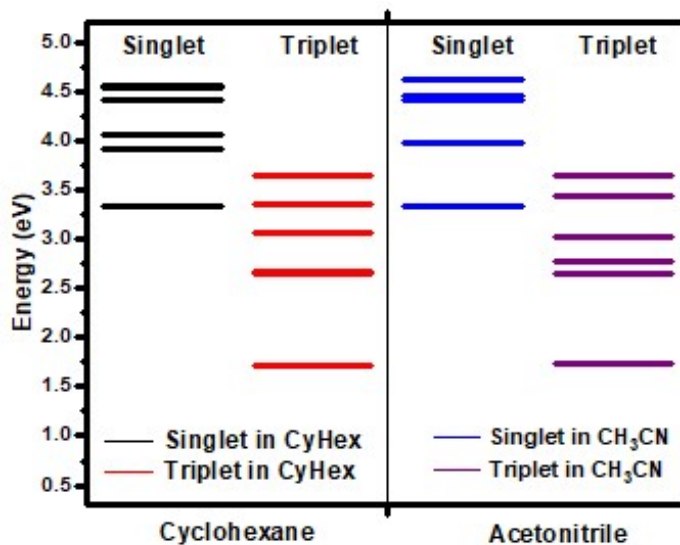

Fig. S24. Shows the computationally calculated singlet triplet energy levels of **BTDPhNO$_2$** in cyclohexane and acetonitrile solvents.

Fig. S25. Lippert mataga plot of (a) **BTDPhNO₂** (b) **BTDPhCN**, (c) **BTDPhCOOMe**, (d) **BTDPh**CHO, (e) **BTDPh**, (f) **BTDPhPh,** (g) **BTDPhᵗBut**, (h) **BTDPhOMe**, and (i) **BTDPhNMe₂** in different solvents.

Fig. S26. (a) Solid state emission spectra of BTD derivatives, and (b) Normalized solid state emission spectra of BTD derivatives. (λ_{ex} at their respective absorption maximum wavelength in cyclohexane solvent).
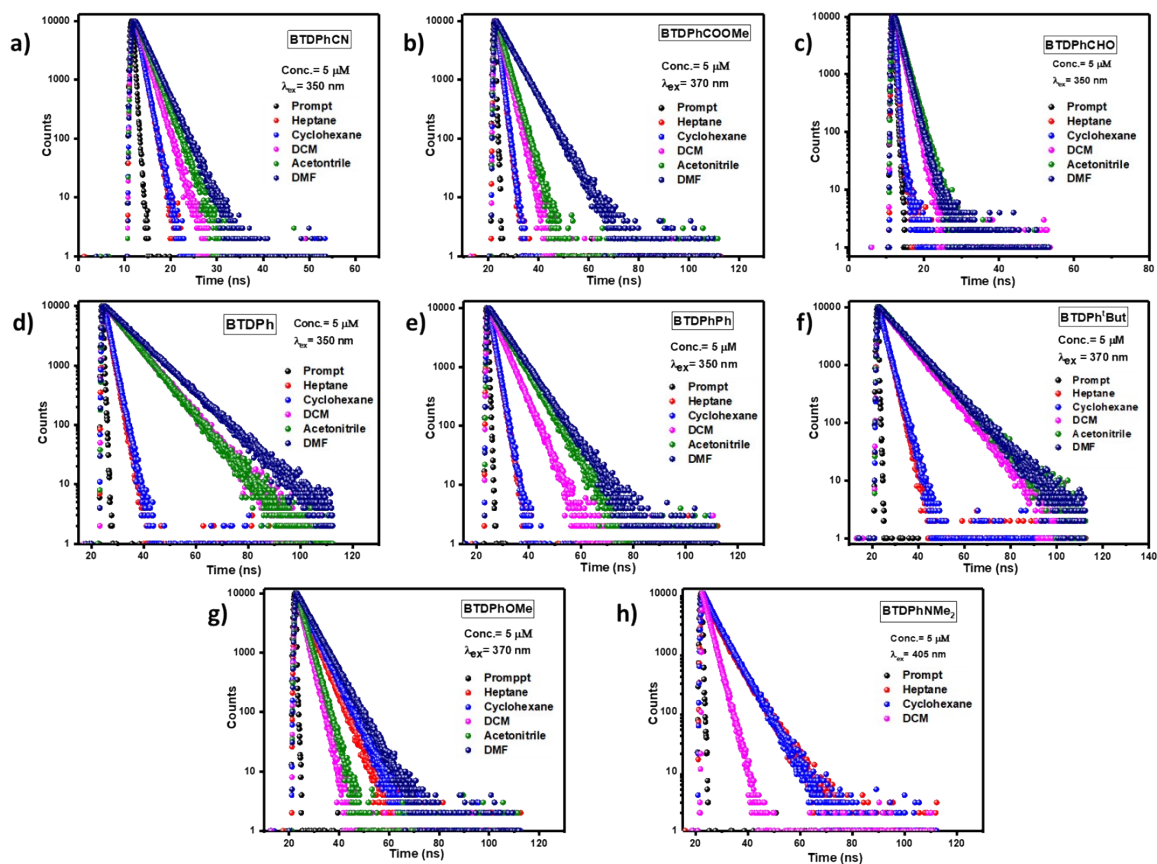
Fig. S27. Fluorescence decay profiles of (a) **BTDPhCN** (λ_{ex} = 350 nm), (b) **BTDPhCOOMe** (λ_{ex} = 370 nm), (c) **BTDPhCHO** (λ_{ex} = 350 nm), (d) **BTDPh** (λ_{ex} = 350 nm), (e) **BTDPhPh** (λ_{ex} = 350 nm), (f) **BTDPh^{t}But** (λ_{ex} = 370 nm), (g) **BTDPhOMe** (λ_{ex} = 370 nm), and (h) **BTDPhNMe$_2$** (λ_{ex} = 405 nm) in solvents of different polarities. ([**BTDs**]=5 x 10^{-6} M)
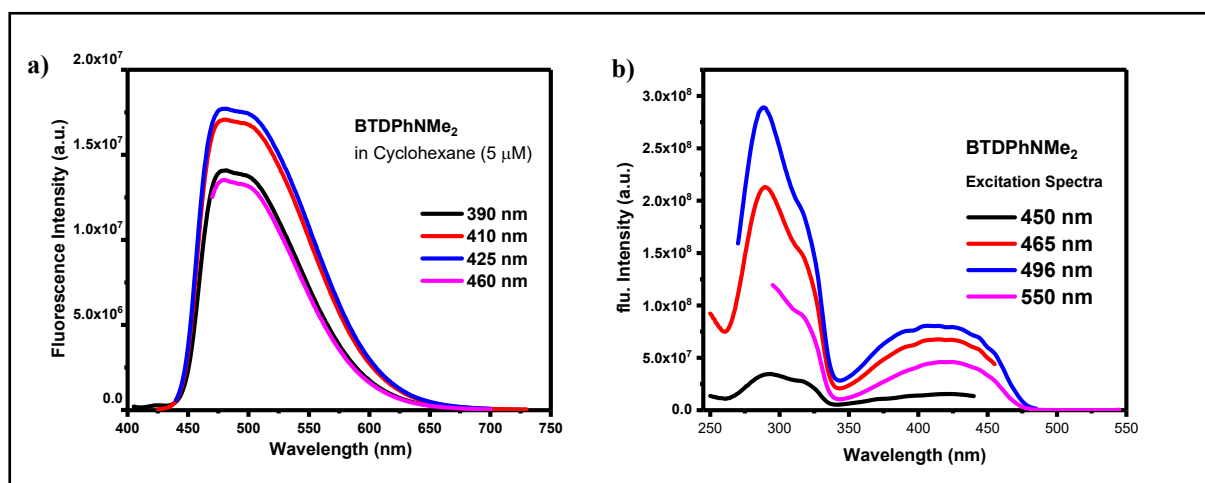
Fig. S28. Shows the (a) the emission spectra, and (b) excitation spectra of **BTDPhNMe$_2$** in cyclohexane, respectively (5 x 10^{-6} M).

Table S7. Fluorescence decay data of **BTDPhNMe$_2$** in cyclohexane of at different λ_{ex} and λ_{em}.

	λ_{em}= 465 nm			λ_{em}= 496 nm			λ_{em}= 555 nm		
	τ_1(ns) (α) (β)	τ_2(ns) (α) (β)	χ^2	τ_1(ns) (α)(β)	τ_2(ns) (α) (β)	χ^2	τ_1(ns) (α) (β)	τ_2(ns) (α) (β)	χ^2
λ_{ex}= 405 nm	3.01 (44) (28)	5.98 (56) (72)	1.27	3.14 (35) (21)	6.08 (65) (79)	1.24	6.20 (100) (100)	--	1.09
λ_{ex}= 450 nm	3.19 (49) (34)	6.07 (51) (66)	1.26	3.01 (35) (21)	6.05 (65) (79)	1.23	6.20 (100) (100)	--	1.28

[a]α is the population of the emitting species, and [b]β is the contribution of each emitting species towards the total emission.

Table S8. Represents the experimental maximum absorption wavelength (λ_{max}, nm) and theoretically [CAM-B3LYP/6-311+g(d,p)] calculated λ_{max}, (in nm), in cyclohexane and acetonitrile of the compounds. . f is the oscillator strength value for the transition $S_0 \rightarrow S_1$.

Compound	Solvent	Energy of Transition (eV)	λ_{max} (theoretical) (nm)	λ_{max} (experimental) (nm)	Oscillator strength (f)	Main Electronic Transitions [weight%]
BTDPhNO$_2$	Cyclohexane	3.3396	371	362	0.8758	HOMO→LUMO (89%) HOMO→LUMO+1 (05%) HOMO-2→LUMO+1 (03%)
	CH$_3$CN	3.3296	372	<u>364</u>	0.9084	HOMO→LUMO (84%) HOMO→LUMO+1 (03%) HOMO-2→LUMO+1 (09%)
BTDPhCN	Cyclohexane	3.3727	368	359	0.7423	HOMO→LUMO (94%)
	CH$_3$CN	3.3914	365	356	0.7134	HOMO→LUMO (94%)
BTDPhCO$_2$Me	Cyclohexane	3.3441	371	365	0.7117	HOMO→LUMO (94%)
	CH$_3$CN	3.3741	358	358	0.6867	HOMO→LUMO (94%)
BTDPhCHO	Cyclohexane	3.3367	372	358	0.7872	HOMO→LUMO (94%)
	CH$_3$CN	3.3571	369	355	0.7680	HOMO→LUMO (94%)
BTDPh	Cyclohexane	3.3276	373	368	0.5221	HOMO→LUMO (94%) HOMO-2→LUMO (03%)
	CH$_3$CN	3.3573	369	365	0.4899	HOMO→LUMO (94%) HOMO-2→LUMO (2.7%)
BTDPhPh	Cyclohexane	3.2498	381	375	0.7586	HOMO→LUMO (88%) HOMO-1→LUMO (09%)
	CH$_3$CN	3.2799	368	368	0.7331	HOMO→LUMO (87%) HOMO-1→LUMO (09%)
BTDPh^{t}But	Cyclohexane	3.2732	379	373	0.5801	HOMO→LUMO (93%) HOMO-2→LUMO (04%)
	CH$_3$CN	3.3041	375	366	0.5502	HOMO→LUMO (93%) HOMO-2→LUMO (4%)

BTDPhOMe	Cyclohexane	3.1961	388	382	0.5679	HOMO→LUMO (91%) HOMO-1→LUMO (07%)
	CH$_3$CN	3.2243	376	375	0.5401	HOMO→LUMO (90%) HOMO-1→LUMO (07%)
BTDPhNMe$_2$	Cyclohexane	2.9654	418	423	0.6633	HOMO→LUMO (86%) HOMO-1→LUMO (11%)
	CH$_3$CN	2.9448	421	421	0.6379	HOMO→LUMO (86%) HOMO-1→LUMO (11%)

Table S9. Theoretically calculated parameters and experimentally observed Lippert-Mataga slope, change in dipole moment ($\Delta\mu$), and fluorescence emission shift from cyclohexane to acetonile ($\Delta\lambda_{em}$) of the **BTDs**.

Compound	BTD PhNO$_2$	BTD PhCN	BTD PhCOOMe	BTD PhsCHO	BTD Ph	BTD PhPh	BTD Ph^{t}But	BTD PhOMe	BTD PhNMe$_2$
Lippert-Mataga Slope	--	4816.7	5638.0	4223.7	7049.2	9795.0	7328.0	12305.0	20871.6
$\Delta\mu$ (D)	--	12.10	15.01	10.50	12.00	22.82	16.13	20.53	26.97
$\Delta\lambda_{em}$ [a] (nm)	15	23	24	23	35	51	45	76	150[b]
q_{CT} (a.u.)	0.555	0.521	0.553	0.485	0.637	0.698	0.693	0.740	0.861
d_{CT} (A°)	3.968	3.165	3.292	2.484	3.753	4.879	4.004	4.562	5.341
t_{index} (Å)	0.306	0.326	0.378	-0.339	01.010	01.346	0.867	1.346	1.884

[a] change in λ_{em} maxima from cyclohexane to acetonitrile. [b] change in λ_{em} maxima from cyclohexane to DCM
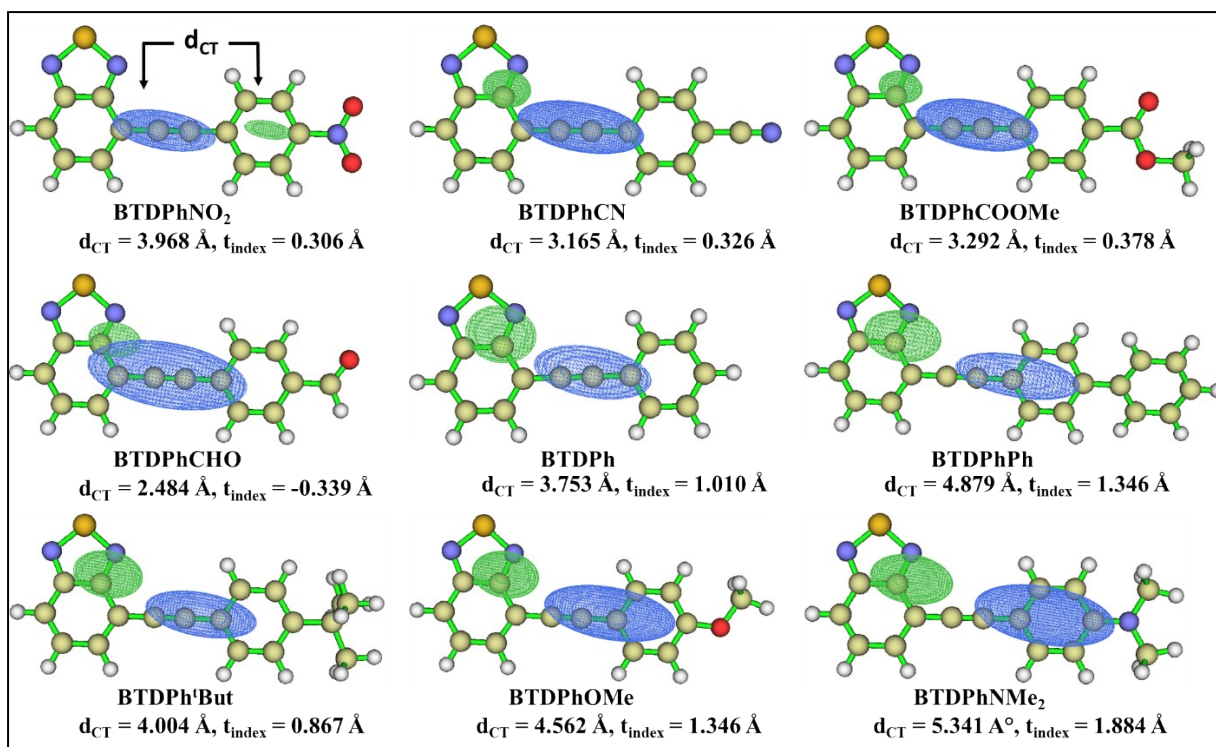
Fig. S29. Plots of positive and negative parts of $\Delta\rho(r)$. Green and blue regions indicate the positive $(\rho+)$ and negative $(\rho-)$ region of $\Delta\rho$ respectively. Different iso-surface values are adjusted so as just to visualize both the regions.

Table S10. Electrochemical properties of the compounds recorded in acetonitrile.

Compound	E_{onset} (ox) (V)	E_{onset} (red) (V)	E_{HOMO}^a (eV)	E_{LUMO}^b (eV)	$E_g^{CV\,c}$ (eV)	$E_g^{opt\,d}$
BTDPhNO$_2$	1.80	-0.84	-6.26	-3.46	2.80	3.02
BTDPhCN	1.53	-1.52	-5.99	-2.78	3.21	3.06
BTDPhCO$_2$Me	1.83	-1.14	-6.29	-3.16	3.13	3.06
BTDPhCHO	1.64	-1.36	-6.10	-2.94	3.16	3.05
BTDPh	1.33	-1.61	-5.79	-2.69	3.10	3.02
BTDPhPh	1.22	-1.54	-5.68	-2.76	2.92	2.95
BTDPh^{t}But	1.21	-1.72	-5.67	-2.58	3.09	2.94
BTDPhOMe	1.08	-1.60	-5.54	-2.70	2.84	2.85
BTDPhNMe$_2$	0.42	-1.62	-4.88	-2.68	2.20	2.43

The first oxidation and reduction of the cyclic voltammograms were considered for the calculations. E_g is the energy gap between HOMO and LUMO and λ_{onset} is the onset of the UV-visible absorption spectra (here taken in acetonitrile). [a] $E_{HOMO} = -[E_{onset} \text{(oxidation)} + 4.8 - E_{FC}]$ eV; [b] $E_{LUMO} = -[E_{onset} \text{(reduction)} + 4.8 - E_{FC}]$ eV; [c] $E_g^{CV} = E_{LUMO} - E_{HOMO}$; [d] $E_g^{opt} = (1240/\lambda_{onset})$ eV

Equation S8. $\qquad E_{HOMO} = -[E_{onset} \text{(oxidation)} + 4.8 - E_{FC}]$ eV

Equation S9. $\qquad E_{LUMO} = -[E_{onset}(\text{reduction}) + 4.8 - E_{FC}] \text{ eV}$

Equation S10. $\qquad E_g^{CV} = E_{LUMO} - E_{HOMO}; \quad E_g^{opt} = (1240/\lambda_{onset}) \text{ eV}$
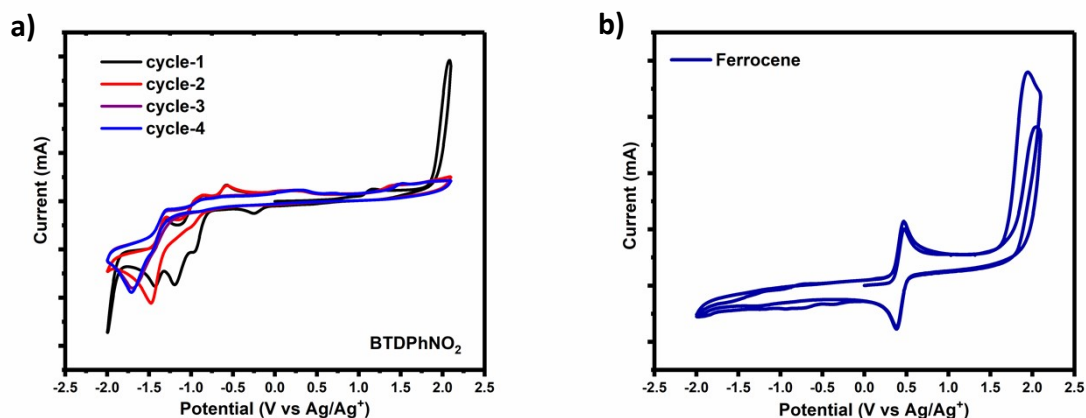
Fig. S30. (a) Cyclic voltammogram of **BTDPhNO₂** for four consecutive cycles in acetonitrile showing its electrochemical instability and (b) Cyclic voltammogram of ferrocene in acetonitrile.
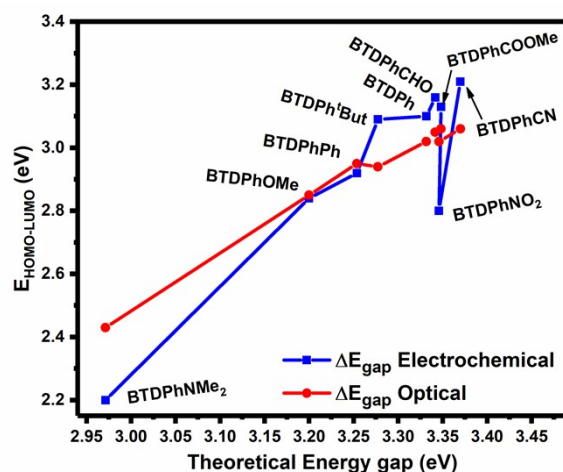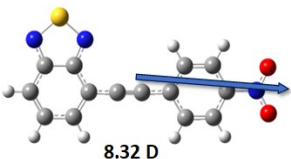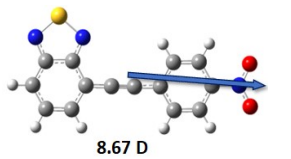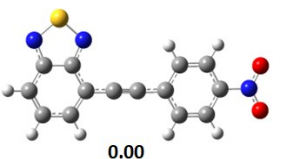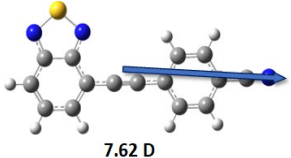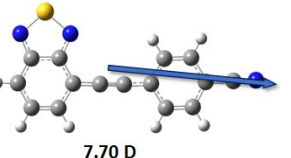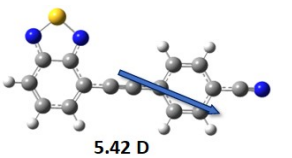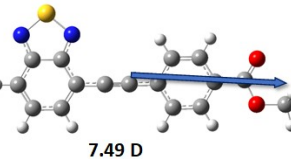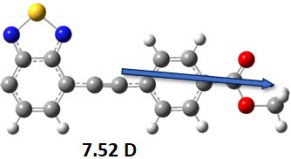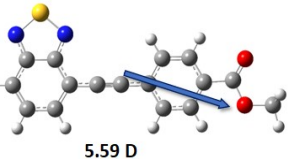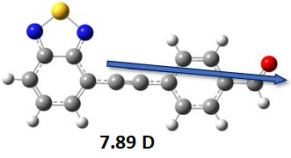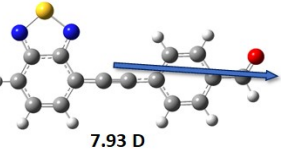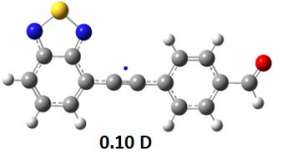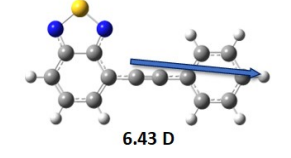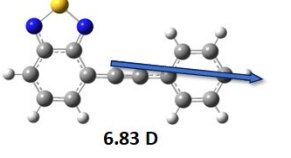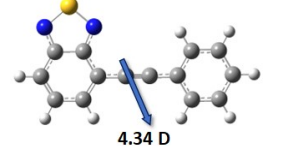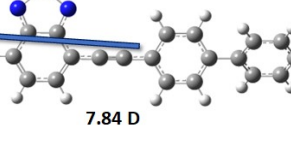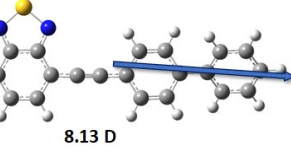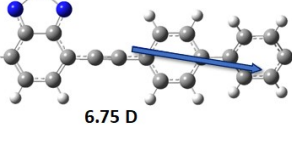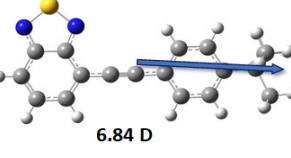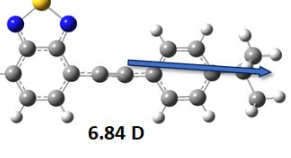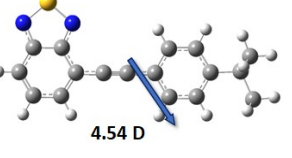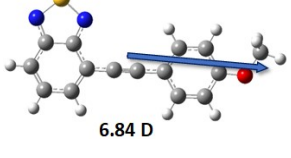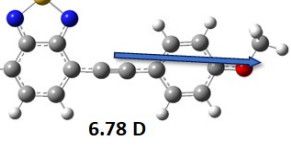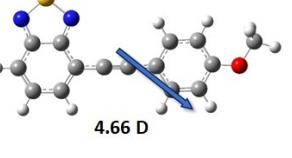

Fig. S31. Comparison of optical and electrochemical energy gap (HOMO-LUMO gap) with respect to the theoretical ones.

Table S11. Calculated transition dipole moment vectors of the compounds (arrows show their directions and their respective magnitudes are written down) for $S_0 \rightarrow S_1$ (absorption), $S_1 \rightarrow S_0$ (emission), and $S_0 \rightarrow S_2$ (absorption) in cyclohexane using CAM-B3LYP/6-311+g(d,p) level of theory.

Compound	Directions of Transition Dipole Moment Vectors and their Magnitudes in Debye (D)		
	$S_0 \rightarrow S_1$	$S_1 \rightarrow S_0$	$S_0 \rightarrow S_2$

32

BTDPhNO₂	8.32 D	8.67 D	0.00
BTDPhCN	7.62 D	7.70 D	5.42 D
BTDPh COOMe	7.49 D	7.52 D	5.59 D
BTDPh CHO	7.89 D	7.93 D	0.10 D
BTDPh	6.43 D	6.83 D	4.34 D
BTDPhPh	7.84 D	8.13 D	6.75 D
BTDPhᵗBut	6.84 D	6.84 D	4.54 D
BTDPhOMe	6.84 D	6.78 D	4.66 D

| BTDPhNMe$_2$ | 7.68 D | 7.26 D | 5.03 D |
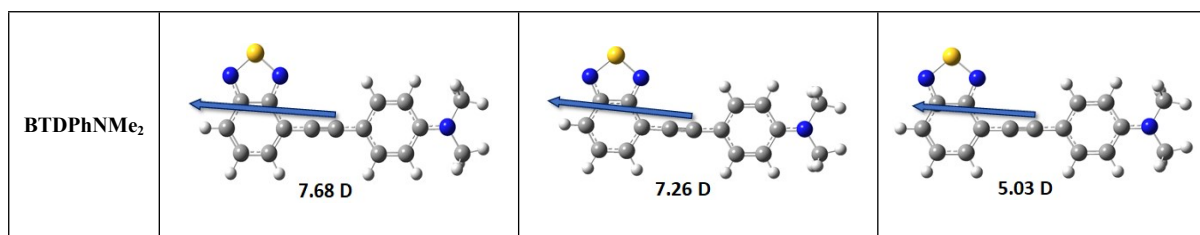
The rotational correlation time (θ) of the fluorophore is given by the following equation.

Equation S11:[6]

$$\theta = \frac{\eta V}{RT}$$

where η is the viscosity, T is the temperature in K, R is the gas constant, and V is the volume of the rotating unit.

References

1. J. G. Calvert, *Pure Appl. Chem.*, 1990, **62**, 2167–2219

2. J. R. Lakowicz, in *Principles of Fluorescence Spectroscopy*, Springer, Third Edit., 2006, p. 192.

3. SADABS, Version 2012/1; Bruker, Bruker AXS Inc.: Madison, Wisconsin, USA, 2012

4. T. Le Bahers, C. Adamo and I. Ciofini, *J. Chem. Theory Comput.*, 2011, **7**, 2498–2506.

5. J. R. Lakowicz, in *Principles of Fluorescence Spectroscopy*, Springer, Third Edit., 2006, p. 363.

6. J. R. Lakowicz, in *Principles of Fluorescence Spectroscopy*, Springer, Third Edit., 2006, p. 367.